DIPLOMARBEIT

Titel der Diplomarbeit

The impact of Influenza A Virus on epithelial cells and macrophages

angestrebter akademischer Grad

Magister der Naturwissenschaften (Mag. rer.nat.)

Verfasser: Christoph Reiser

Studienrichtung: A441, Biologie – Stzw. Genetik - Mikrobiologie

Betreuer / Betreuerin: Prof. Dr. Thomas Decker

                             Dr. Amanda M. Jamieson

Wien, am 14.Juni.2010

Table of contents

Abstract

Influenza A virus is the most relevant clinical pathogen of the orthomoyxoviridae family for humans. It is known to predispose the lung to secondary bacterial infections which lead to bacterial pneumonia. Usually infection with influenza virus causes an increase in bacterial load, however, coinfection of mice with influenza and *Legionella pneumophila* leads to immunopathology without an increase in pathogen burden. Investigating possible mechanisms for this immunopathology was our main interest. TNFα known to cause immunopathology, was elevated after the bacterial infection. We therefore wanted to look at the effect of TNFα on influenza infected lung epithelial cells. The results showed us a clear synergism suggesting an important role of TNFα during coinfections. Zinc, known to be a cytoprotectant and anti-apoptotic agent, was used to investigate a possible impact on the cell survival during infection with influenza virus combined with TNFα. A rescue of the synergistic effect could not be seen in our results. Another possibility for the increase in immunopathology is an inefficient uptake of dead cells by infected macrophages, which would lead to an increased release of pro-inflammatory cytokines. Therefore, infected macrophages and uninfected macrophages were compared for their ability to phagocytose influenza A virus infected or apoptotic cells. These results suggest strongly that macrophages are

directly affected by influenza A virus infection *in vitro*. In addition, observation of macrophages by live imaging revealed an altered motility upon infection with influenza virus.

Zusammenfassung

Influenza A Virus ist das für den Menschen relevanteste klinische Pathogen der orthomyxoviridea Familie. Es ist bekannt dafür die Lungen anfälliger für sekundäre Bakterielle Infektionen zu machen, die bakterielle Lungenentzündungen auslösen. Während einer Coinfektion mit Influenza steigt normalerweise die Anzahl an Bakterien. Dies ist jedoch nicht der Fall bei einer Coinfektion von Influenza mit *Legionella pneumophila.* Hierbei kommt es zu einer Immunpathologie, ohne einen Anstieg der bakteriellen Belastung. Unsere Untersuchungen umfassen unterschiedlicher Mechanismen, die zu dieser Immunpathologie führen könnten. TNFα, bekannt dafür Immunpathologie auszulösen, ist nach der bakteriellen Infektion erhöht. Aus diesem Grund wollten wir in Erfahrung bringen, was für einen Effekt TNFα auf Influenza infizierte Zellen hat. Die Ergebnisse zeigen uns einen klaren Synergismus, der eine wichtige Rolle von TNFα während Coinfektionen nahe legt. Zink, bekannt für seine Zellschützende und anti-apoptotische Funktion, wurde verwendet, um eine mögliche Rolle für das Überleben der Zellen während einer Influenza Infektion zusammen mit TNFα zu analysieren. Unsere Ergebnisse konnten keine Reduktion des Synergismus aufzeigen. Eine weitere Möglichkeit der erhöhten Immunpathology ist die unzureichende Aufnahme von toten Zellen durch infizierte

Makrophagen, welche eine erhöhte Freisetzung von pro-inflammatorischen Zytokinen zur Folge hätte. Aus diesem Grund wurden infizierte und uninfizierte Makrophagen in ihrer Fähigkeit verglichen, Influenza infizierte oder tote Zellen zu phagozytieren. Die Ergebnisse legen nahe, das eine Influenza A Virus Infektion *in vitro* einen direkten Einfluß auf Makrophagen hat. Weiters konnte während der Observation von Makrophagen bei Lebendzellbeobachtungs-Experimenten, ein veränderter Bewegungsablauf durch eine Infektion mit Influenza beobachtet werden.

1 Introduction

1.1 Influenza

Influenza A Virus (IAV) is a negative sense, single stranded RNA virus of the orthomoyxoviridae family. The RNA consists of 8 segments encoding 11 proteins (1) (Figure 1). Influenza is known to cause respiratory diseases by mainly infecting respiratory epithelial cells from where on the infection can spread to alveolar macrophages (2).
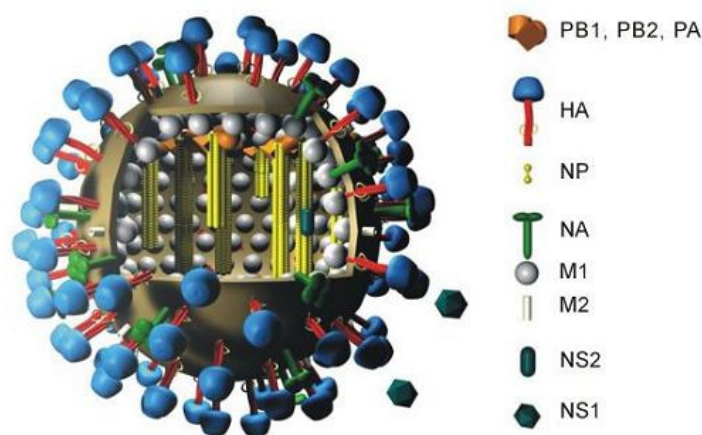
Figure 1: Structure of an IAV showing its various proteins. Image copyright by Dr. Markus Eickmann, Institute for Virology, Marburg, Germany

Source: http://www.influenzareport.com/ir/virol.htm

The infectious route of the virus is through binding of the viral surface protein hemagglutinin (HA) to sialic acid sugars on their target cells (1-3). It is then taken up in an endosome from where the virus is able to release its viral
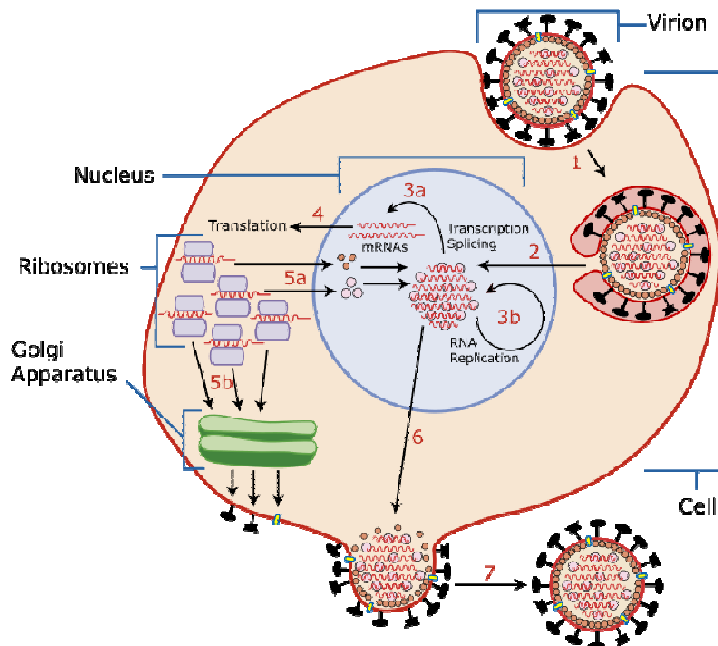
Figure 2: Shows the route of infection from an influenza Virus in an epithelial cell. Virus binds with hemagglutinin (HA) to the cell and gets taken up [1]. Release of the viral RNA and RNA polymerase into the cytoplasma from where it gets transported into the nucleus [2]. Transcription/replication of the RNA in the nucleus [3a/3b]. Translation of the mRNA in the cytoplasma [4]. Secretion of HA and neuroaminidase (NA) via Golgi apparatus to the cell surface [5b]. Viral proteins get transported back into the nucleus to bind viral RNA [5a]. Viral RNA and core proteins leave nucleus and enter a formed bulge [6]. The virus buds off from the cell with the help of neuroaminidase which cuts the sialic acid sugars on the cell surface [7].

Source:

http://www.ncbi.nlm.nih.gov/genomes/GenomesHome.cgi?taxid=10239&hopt=scheme

RNA, accessory proteins and RNA polymerase into the cytoplasm (4; 5). A complex is formed which then is transported into the nucleus where the transcription and replication of the RNA takes place (6). The transcribed mRNA is transported to the ribosomes in the cytoplasm. Once the proteins are translated they either get secreted via the Golgi apparatus to the cell surface (HA, neuroaminidase

(NA) and M2) or transported back into the nucleus to bind the replicated viral RNA (7). The newly replicated negative stranded RNA, RNA polymerase and other viral proteins leave the nucleus to enter a bulge in the cell that has been created by a cluster of HA, NA and M2 molecules to form a new virus particle. This is budded off from the cell by cutting the sialic acid sugars with the NA (3; 8) (Figure 2). After influenza has kept the cell alive long enough to propagate enough new viruses, it induces an apoptotic cell death of the infected cell (9-11).

1.2 Immune response to influenza

A very strong inflammatory response accompanies a normal influenza infection (12). The first step of the innate immune response is the destruction of infected cells by natural killer (NK) cells and the production of cytokines including IFN-α/β (13; 14). Type I IFNs are released by infected epithelial cells and macrophages, functioning to directly induce an antiviral state. Further they enhance the host immune response by upregulation of the gene expression of pro-inflammatory cytokines and MHC-class I complexes (15). The pro-inflammatory cytokines (TNFα, IL-1β, IL-6) and chemokines (MCP-1, RANTES, MIP-1α/β, IP-10, IL-8 (in humans only)) (16; 17; 13) favour the extravasation of blood monocytes and the further development of antiviral and Th1-type immune response (13). For further protection against infection, B-cells produce antibodies against the cell surface HA and NA to neutralize free viruses by inhibiting the

binding and entry into cells (18). To eradicate already established infections CD8$^+$ cytotoxic T-cells (CTL) cells work as the main cellular source, that seek and destroy already infected cells (14) (Figure 3).
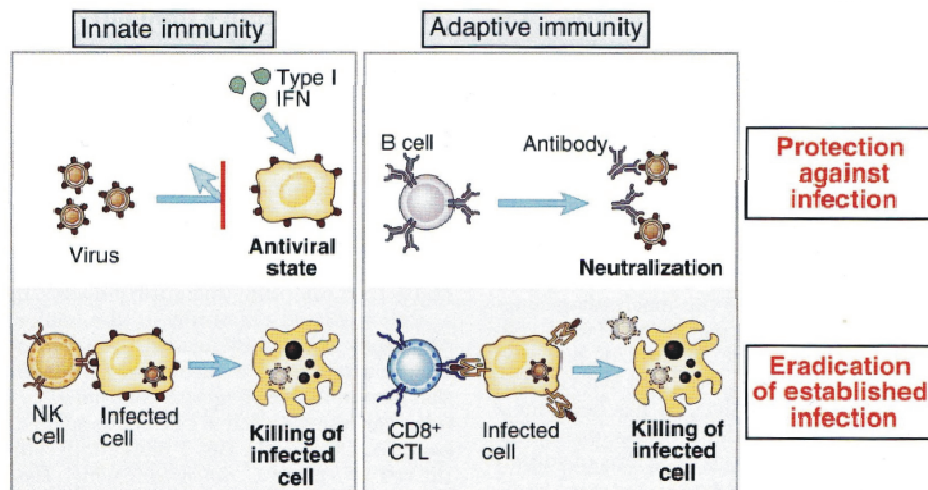
Figure 3: Innate and adaptive immune responses against viruses.

Source: Abul K. Abbas, Cellular and molecular immunology, fifth edition; 2005

1.3 Coinfections

As recent studies have shown, the high mortality rate of some of the great pandemics of history like the Spanish flu can possibly be linked to a secondary bacterial infection, causing bacterial pneumonia (19; 20). There are many mechanisms for the influenza virus to predispose the lung to bacterial infections. One of the mechanisms is the inhibition of NK cell activity by the influenza virus infection (21), for example, resulting in an impaired NK cell response to subsequent *Staphylococcus aureus* infection (22).

Another very important mechanism is increased adherence of bacteria to the host cell (23; 24). In the case of *Streptococcus pneumoniae* this is achieved by the influenza NA, which cuts off the sialic acid, leaving more space for bacterial binding sites (25). The result is a higher bacterial titer and an increased death in mouse models of coinfection (26; 27). For *Streptococcus pyogenes* it has been reported that the HA, which is expressed on the cell surface of influenza infected cells, promotes internalization of the bacteria. This leads to high death rate of the coinfected mice (28).

An overreaction of the host immune response with an excessive cytokine production that results in immunopathology (29; 30) but no increase in bacterial burden can be seen in coinfected mice with *Legionella pneumophila.* The increase in the local inflammatory response includes the pro-inflammatory cytokines IL-6, IL-1β and TNFα. Also a clear increase in damage to the lung epithelium is present when looking at lung sections (31) (Figure 4). We therefore became interested in studying this phenomenon.

Figure 4: Lung sections were stained by H&E and scored to look at epithelium damage.

Source: Amanda M. Jamieson, R. J. H. a. R. M., *Respiratory co-infection with influenza virus and Legionella pneumophila results in rapid lethal infectious pneumonitis.* 2009. (unpublished manuscript)
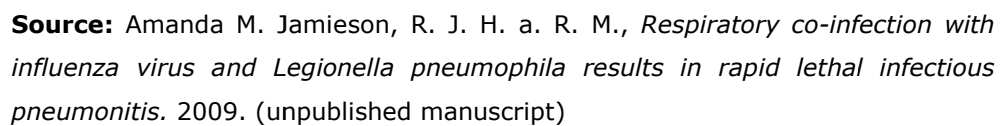
2 Aims

We wanted to examine the reason for the immunopathology induced by *L. pneumophila* after a primary influenza infection. TNFα, elevated after the bacterial infection and known to cause immunopathology, became our main interest. Therefore we looked at the effect TNFα has on influenza infected lung epithelial cells. Zinc, known to be a cytoprotectant and anti-apoptotic agent (32; 33), was further used to try and counteract the increased cell death that we were able to see. Looking for the cause of elevated numbers of pro-inflammatory cytokines, macrophages were examined. Their ability to phagocytose apoptotic and infected cells is extremely important (34). A possible defect in the phagocytic ability of macrophages during an influenza virus infection would lead to an increased number of dead cells that turn secondary necrotic (35). The outcome is an increased pro-inflammatory release of these cells and might be the cause of the immunopathology that we see. To find other impacts of the viral infection on the functionality of macrophages, we observed their movement behaviour by live imaging.

3 Project 1 – Influenza and TNFα

3.1 Introduction

During a coinfection with *L. pneumophila*, TNFα is one of the pro-inflammatory cytokines that is increased (31). The main pathways activated by TNFα are NFκB, JNK, p38-MAPK and induction of cell death (36; 37) (Figure 5).

The possibilities of cross-talk between the different pathways and the capability of inducing necrotic or apoptotic cell death, leading to extensive tissue damage, focused our interest on TNFα. We did experiments *in vitro* with cell lines and primary lung epithelial cells, using TNFα to mimic the secondary bacterial infection of *L. pneumophila*. We observed cell death induced by addition of TNFα before, at the same time and after Influenza A Virus (IAV) infection. What we saw is that IAV leads to an increased cell death after a subsequent TNFα addition.

We examined a possible role for zinc in the increased cell death seen in coinfected epithelial cells. It is a well known cytoprotectant and anti apoptotic agent (32; 33) though too high concentrations may lead to cytoxicity (39). During normal bacterial infections a reduction in zinc levels correlates with optimal immune reaction and reduced virulence by the bacterial pathogen (40). However, prolonged reduction in zinc is also associated with a reduced immune function by impaired cytokine production,

predisposition to apoptosis (41) and a decreased T-cell (40) and B-cell function (42).
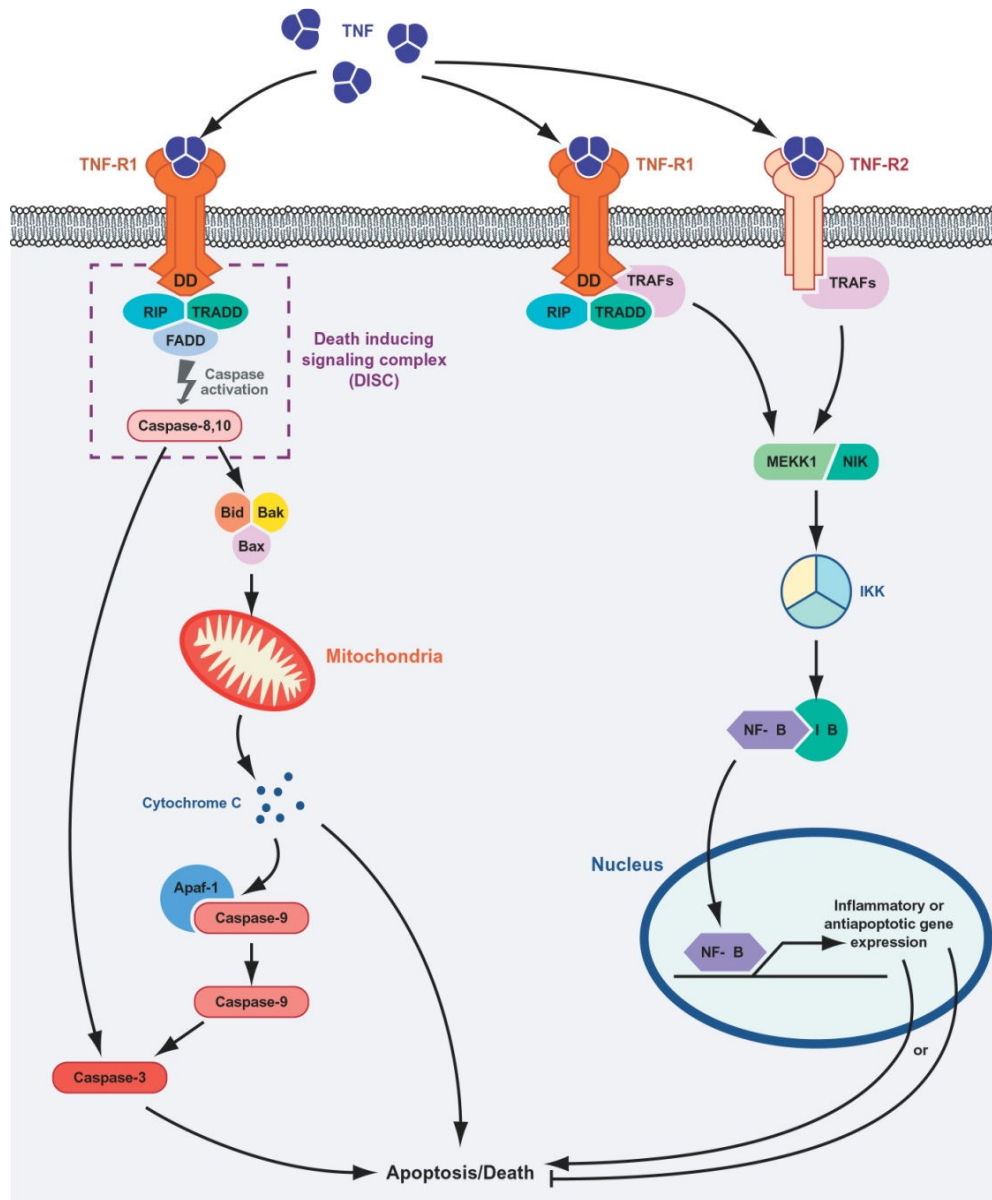
Figure 5: TNFα and its different inducable pathways leading either to antiapoptotic gene expression or to induction of cell death. **(38)**

Source: Rahman MM, McFadden G. *Modulation of Tumor Necrosis Factor by Microbial Pathogens*. PLoS Pathog 2006 Feb;2[2]

Concerning influenza, zinc has a direct inhibitory impact on the viral triggered apoptotic pathways (43; 44). Given that zinc can reduce influenza virus pathology, a reduction of the zinc levels after a bacterial infection might again increase its pathology due to a loss of the inhibitory functions of zinc (41). Pre-treatment, depletion and simultaneous addition of zinc to IAV infected and TNFα treated cells showed us indeed a higher cell death by depletion of zinc in single treated IAV cells. No rescue of cell death in cotreated cells could be seen.

3.2 Results

3.2.1 Cytotoxicity of Influenza and TNFα in cell lines

Our focus lay on the analysis of the cell death that is induced in cells having an IAV infection and the subsequent reaction of these infected cells to the pro-inflammatory cytokine TNFα. The experiments were done with the human A549 lung epithelial cell line and the mouse LL/2, MLE12, MLE15 cell lines. This was done to have a broad overview of this effect and to be able to compare the differences that might occur, especially between mouse and human. Due to differences in growth speed of the cell lines, the cell amount for the start of the experiment was determined to have 10.000 cells for A549, MLE12 and MLE15 per well, while the LL/2 received 5.000 cells per well (data not shown).

The first experiment of interest was to see the effect that different doses of TNFα would have on virus infected cells. LDH-Assay (45) revealed that TNFα addition increases the percentage of dead cells during an infection. A titration of TNFα led to a continuously lower cell death percentage in mouse cell lines (Figure 6) as well as in the human cell line. (Figure 7) An additional PI staining was done in parallel to the LDH-Assay for the LL/2 cell line that gave a similar result (Figure 8).

Figure 6: Mouse cell lines LL/2, MLE12 and MLE15 induced with different doses of TNFα, 5 hours after the virus infection. Experiments were analyzed with an LDH-Assay. Data is representative of two independent experiments with three replicates in each group.

Figure 7: Human cell line A549 induced with different doses of TNFα, 5 hours after the virus infection. Experiments were analyzed with an LDH-Assay. Data is representative of two independent experiments with three replicates in each group.

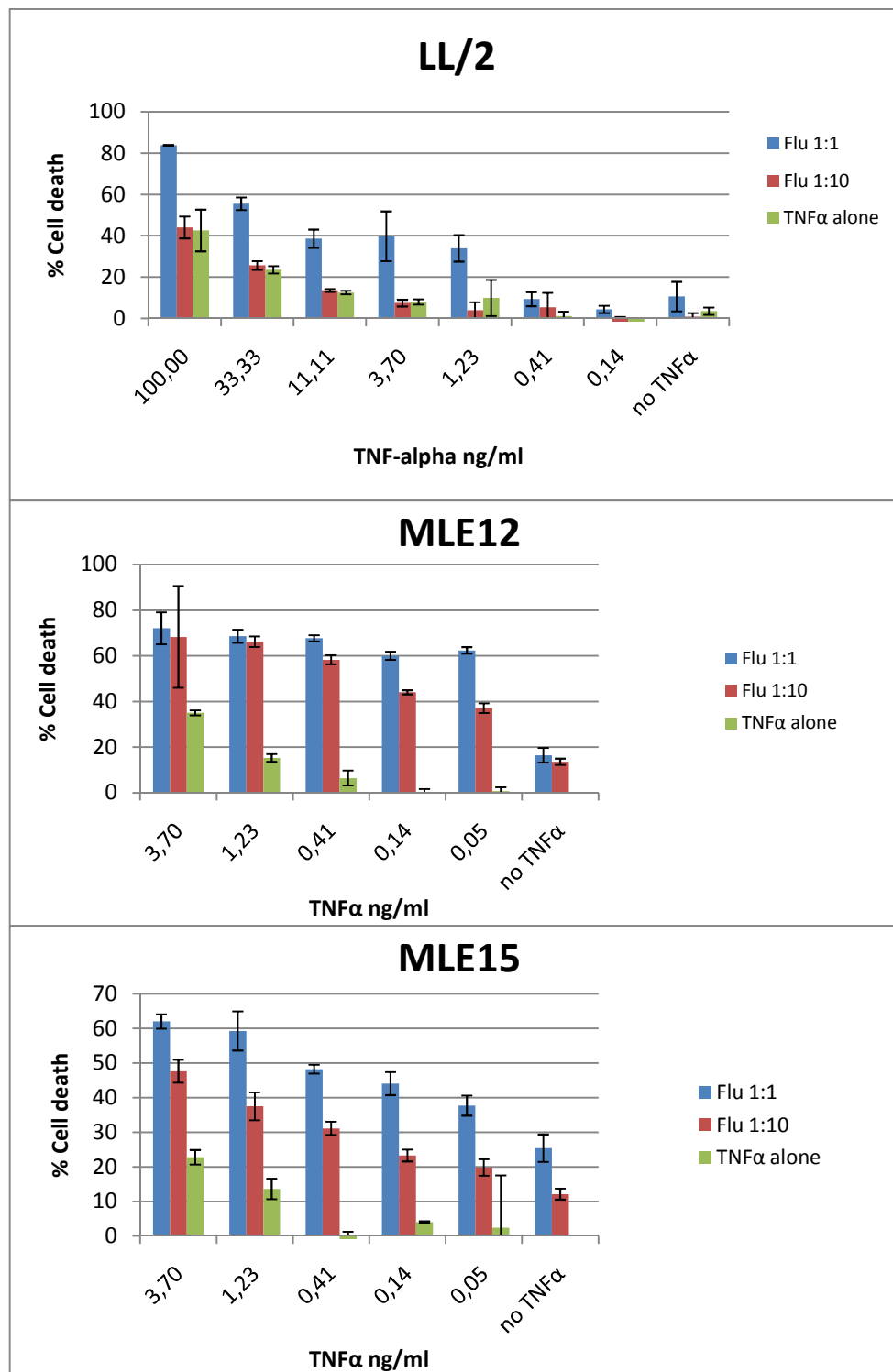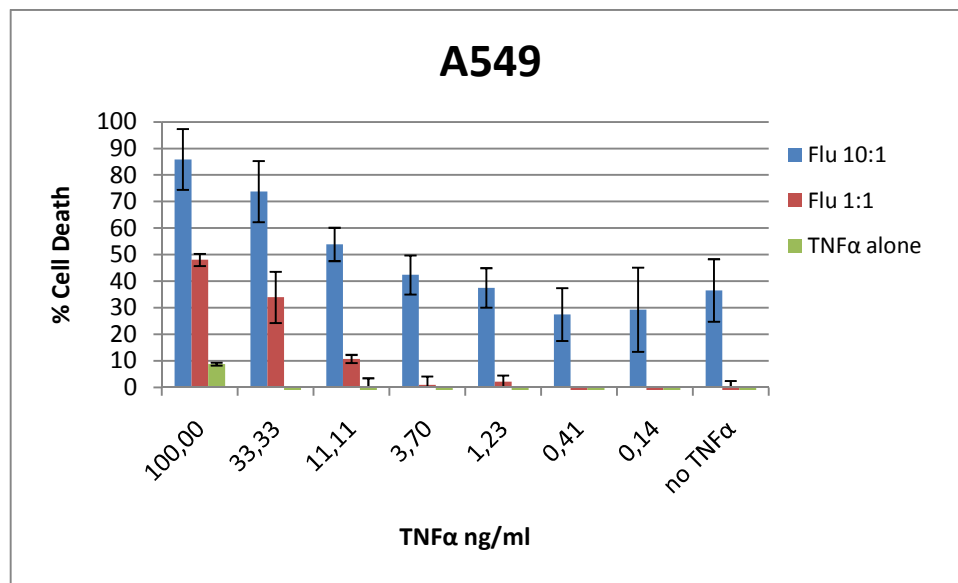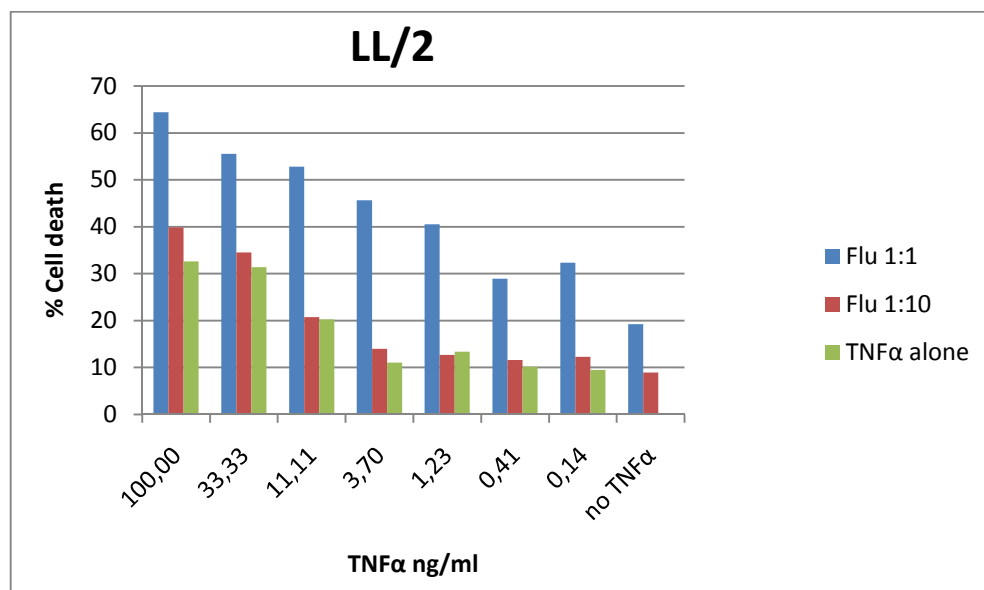**Figure 8:** Mouse cell line LL/2 induced with different doses of TNFα, 5 hours after the virus infection. Experiments were analyzed with PI staining. Data is from one experiment with one sample in each group.

If we focus now on the difference that we see between the highest amount of TNFα alone, the highest infection with IAV alone and the co treatment, the outcome is striking. All four cell lines have a synergistic increase in cell death by cotreatment with IAV and TNFα addition after 5 hours (Figure 9). Looking at the TNFα induction alone we are able to see that all four cell lines react differently, having only 10% cell death with our human cell line A549. The mouse LL/2 cells in contrast had a high cell death of 40% with the highest amount of TNFα. IAV infection alone shows differences as well. The human cell line being more robust against the TNFα, also needs a higher amount of IAV to see cell death during the infection. Both differences are very likely due to the use of mouse TNFα and mouse adapted influenza A virus for all cell lines. No increase in cell death above the normal TNFα cell death level can be observed in the LL/2 with the lower IAV infection. This indicates that it is below an effective virus infection (Figure 6).
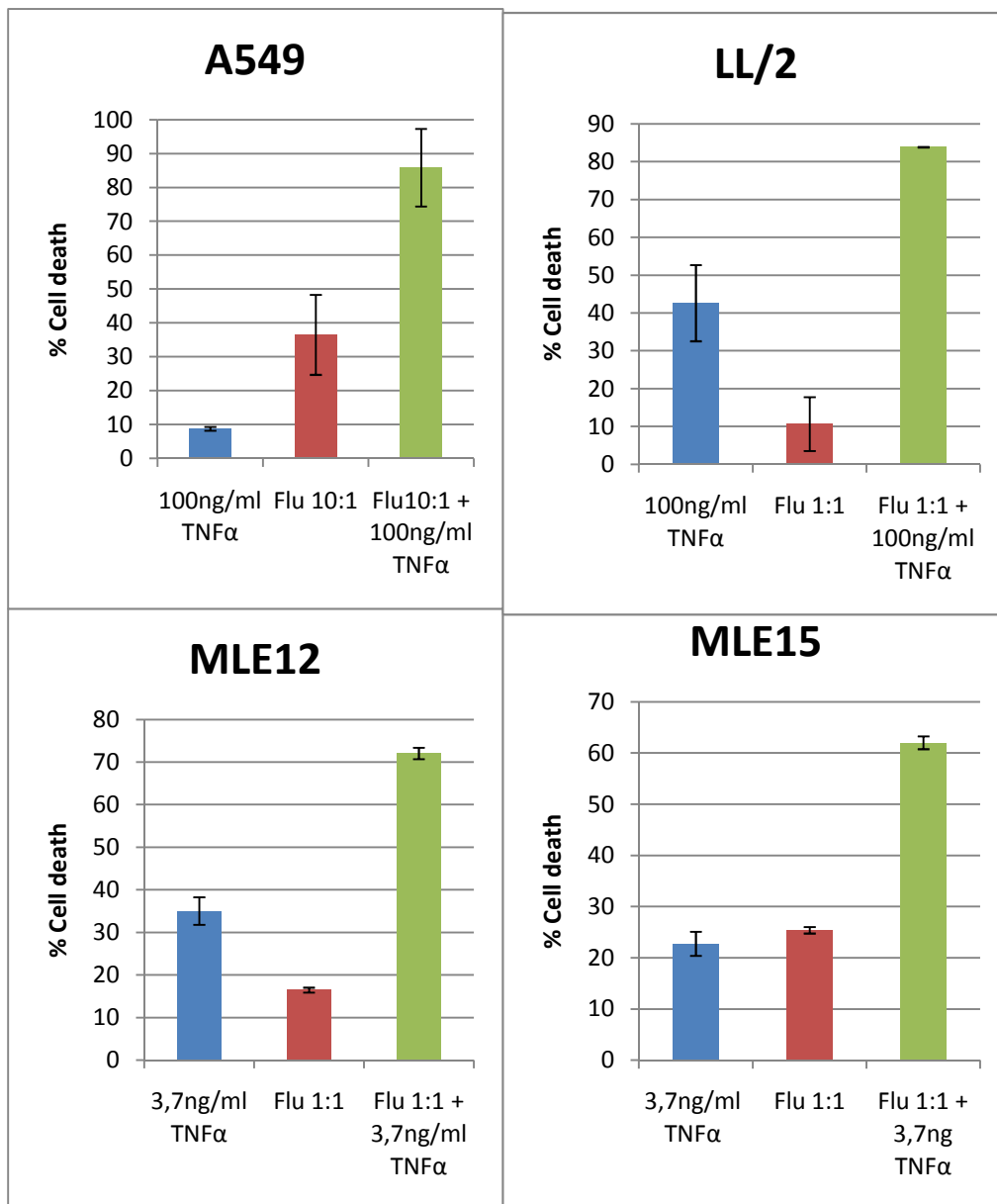
Figure 9: Comparing the effect of the highest induced TNFα alone, the highest infection with IAV alone and the co treated cells which had TNFα added 5h after the IAV infection. A synergistic effect in the co treated cells can be seen with an immense increase of the percentage in cell death. Data is representative of two independent experiments with three replicates in each group.

3.2.2 Different timepoints of TNFα addition

The synergistic effect was seen at the given time point after adding TNFα 5h after the infection. We then wanted to know if the addition of TNFα 5h before or at the same time as the virus infection would lead to a different outcome. First we analyzed the ability of LL/2 and A549 if they were able to express TNFα themselves, which would nullify the relevance of adding TNFα at different time points. Previous studies have suggested that mouse bronchoalveolar epithelial cells do express TNFα but wane after a while (46) while others state that they are in general poor producers (47). Our findings though showed that there was no additional production of TNFα visible in the infected cell lines compared to uninfected (Figure 10).
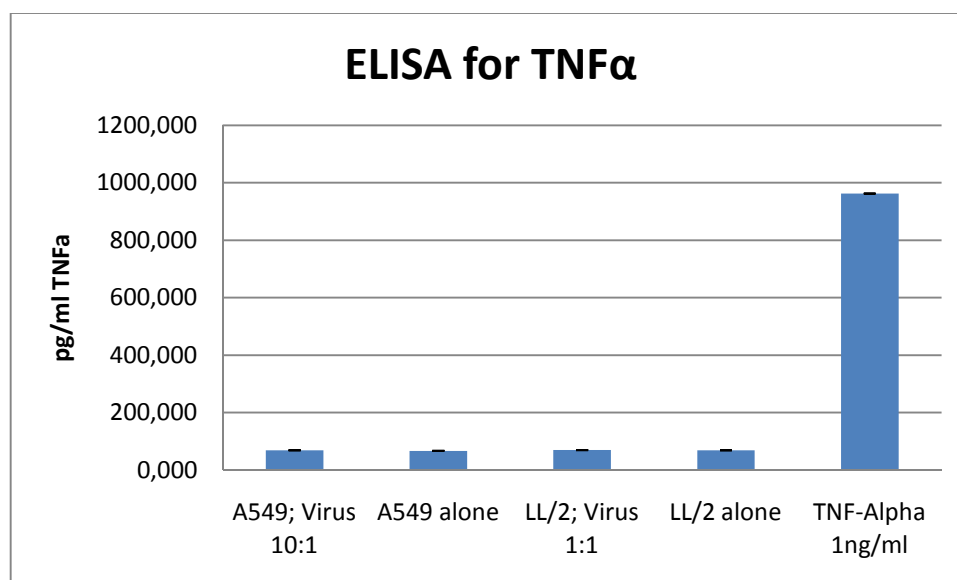
Figure 10: ELISA analyses for TNFα in the cell lines LL/2 and A549. The difference between infected cell line and uninfected cell line was compared to check for activation of TNFα. Data is representative of one experiment with three replicates in each group.

Adddition of TNFα 5h after the IAV infection led to a synergistic increase, while addition of TNFα at earlier time points did not. The addition 5h before or at the same time did not change the percentage in cell death (Figure 11).
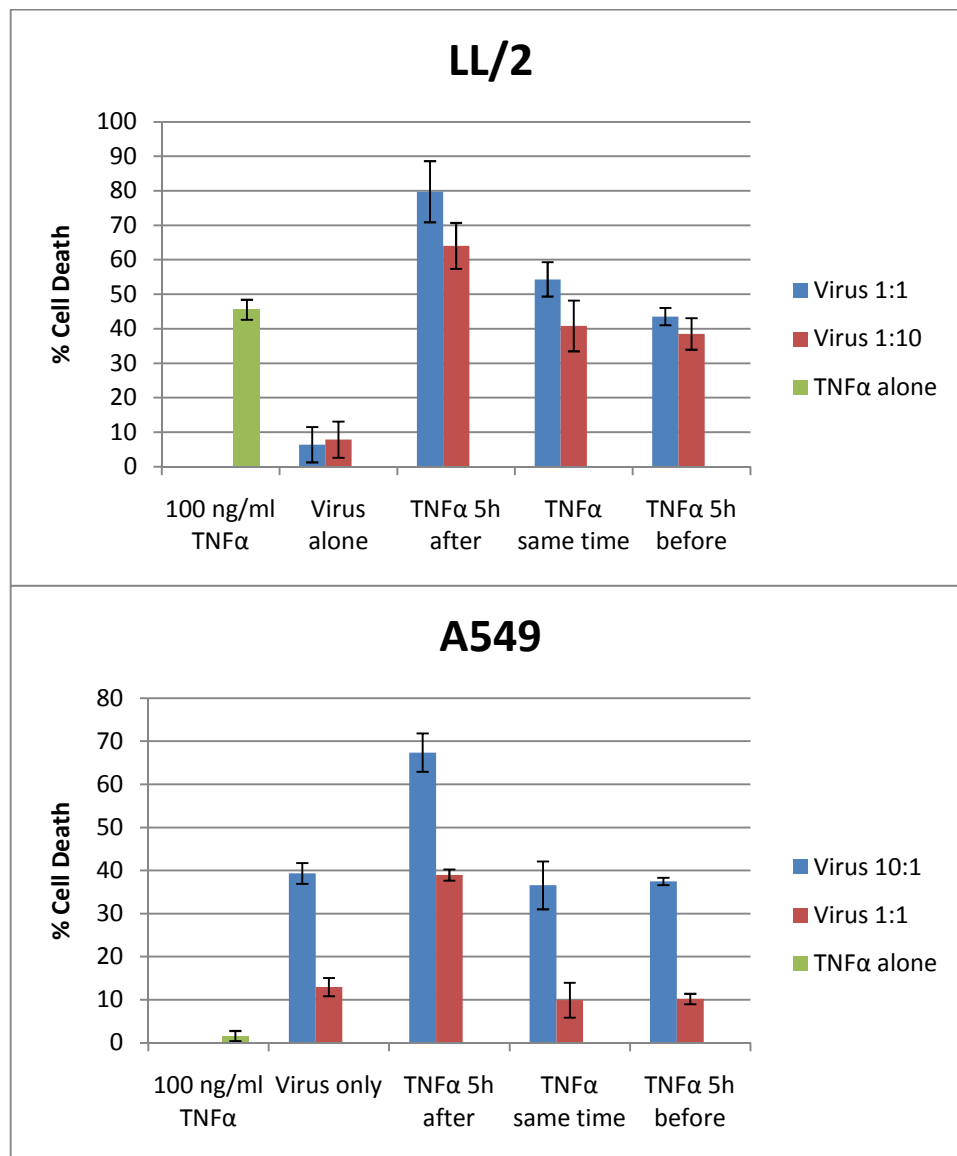
Figure 11: Looking at different time points of TNFα addition in LL/2 and A549 cells. Only if TNFα is added 5h after the virus infection a synergism can be observed. The addition of TNFα 5h before or at the same time as the virus infection leads to no changes in the percentage of cell death compared to TNFα alone or IAV alone. Data is representative of one experiment with three replicates in each group.

3.2.3 Cytotoxicity of Influenza and TNFα in primary cells

The synergistic effect of influenza virus and TNFα is consistent in all cell lines tested so we examined primary lung epithelial cells (LECs). After isolation we checked for the purity of the LECs to be sure that no immune cells were present during our experiment (Figure 12). All the cells expressed E-cadherin, a marker for epithelial cells, demonstrating a high degree of purity (48).
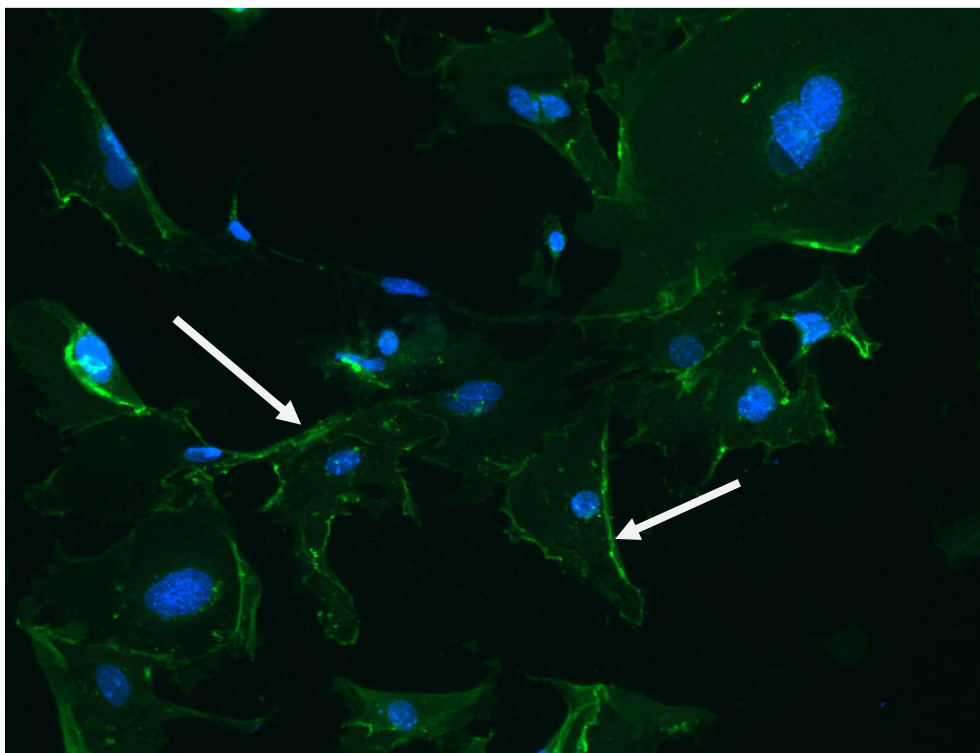
Figure 12: Staining for LECs by DAPI (blue) and FITC-e-cadherin (green). Dense green lines between cells are accumulated e-cadherin (white arrows), which is needed for cell-cell adhesion.

Using these cells to look at cell death led to complicated results. A 24-well plate showed us no negative or synergistic effect by the addition of TNFα (Figure 13). The

setup of a 96-well plate showed us the same synergistic result that we were able to see with our cell lines (Figure 14).

Figure 13: Primary lung epithelial cells being treated with IAV and TNFα in a 24-well plate setup. The setup shows a reduction in cell death in IAV and TNFα treated cells. Data is representative of two independent experiments with one sample in each group.

Figure 14: Primary lung epithelial cells being treated with IAV and TNFα in a 96-well plate setup. The setup shows a synergistic effect of IAV and TNFα treated cells. Data is representative of one experiment with three replicates in each group.

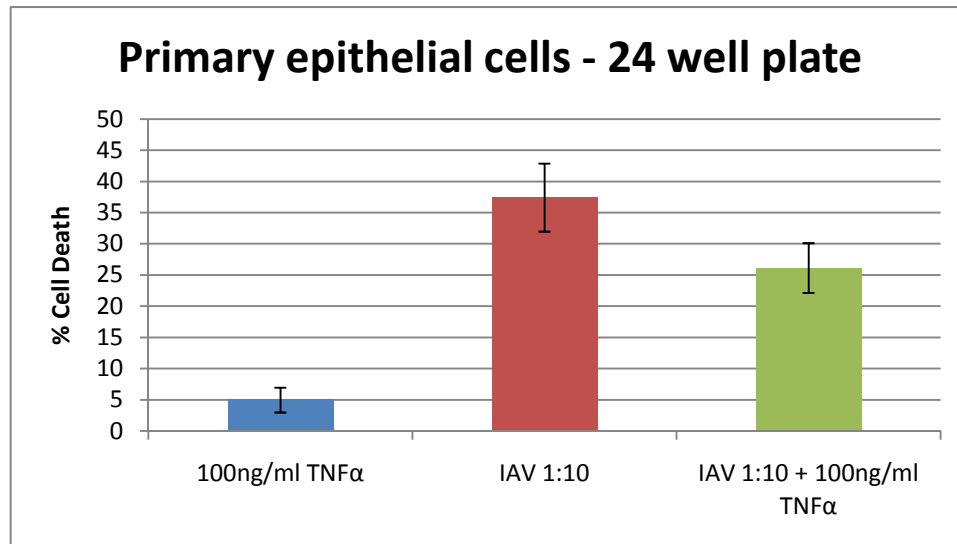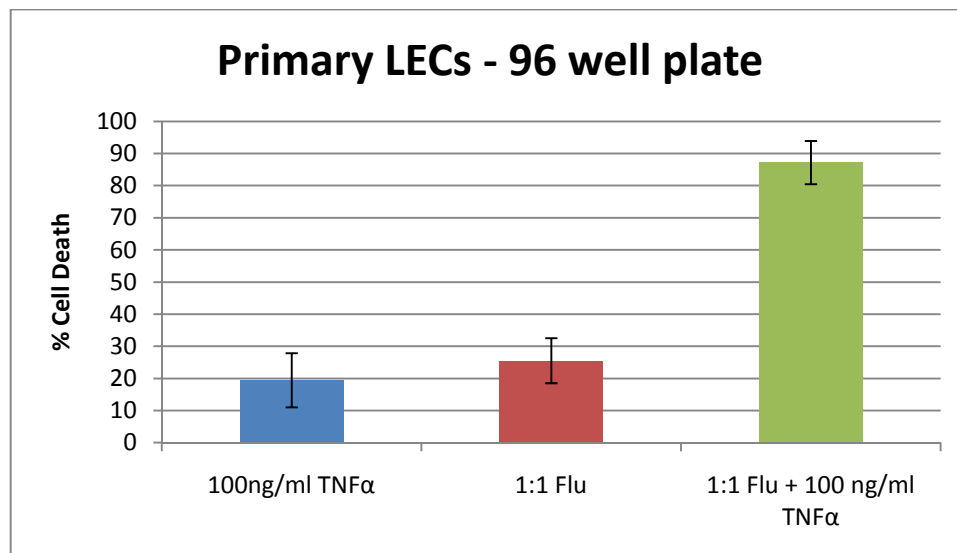Even a lower dose of IAV induced more cell death in the 24-well setup compared to the higher IAV in the 96-well setup. The TNFα induced cell death was four times lower in the 24-well setup than in the 96-well setup. Observing the cell density between both setups, 100 000 cells were more dense in the 24-wells than 10 000 cells were in the 96-wells. This could be one reason for the different outcome.

3.2.4 The impact of zinc on cell survival

As mentioned in 3.1, zinc is known to be a cytoprotectant and an anti-apoptotic agent (32; 33) that enhances cell survival during infections (42). We therefore wanted to see if we can rescue the synergistic cell death that we were able to see with IAV and TNFα treatment.

After determining the optimal concentrations of zinc for the cell lines we started our experiments (data not shown). Two setups were used to analyse the effect of zinc. The first setup had zinc pre-treated cells that received the zinc the night before the viral infection. With the second setup the cells received zinc only at the same time, as the viral infection occurred. Comparing the two setups showed us, that the earlier zinc is introduced to the cells, the more it helps the general survival of them. This could be observed by a reduced cell death of the zinc pre-treated cells compared to the cells that received zinc at a later time point (Figure 15). Zinc pre-treated cells had the lowest amount of cell death from all the experiments. Therefore the data was normalized to those cells.

Comparing the other treatments for changes in cell death gave us following results. Depleting the zinc after pre-treating the cells with it and subsequently adding IAV alone or TNFα alone, led to a higher cell death in the cell lines compared to the cells that did not have any zinc at all. The stress induced due to the depletion might be the cause for that. However looking at the combined IAV and TNFα treated cells, we are neither able to see an increase of cell death after depletion of zinc, nor are we able to see a reduction in the percentage of cell death in the presence of zinc (Figure 15).
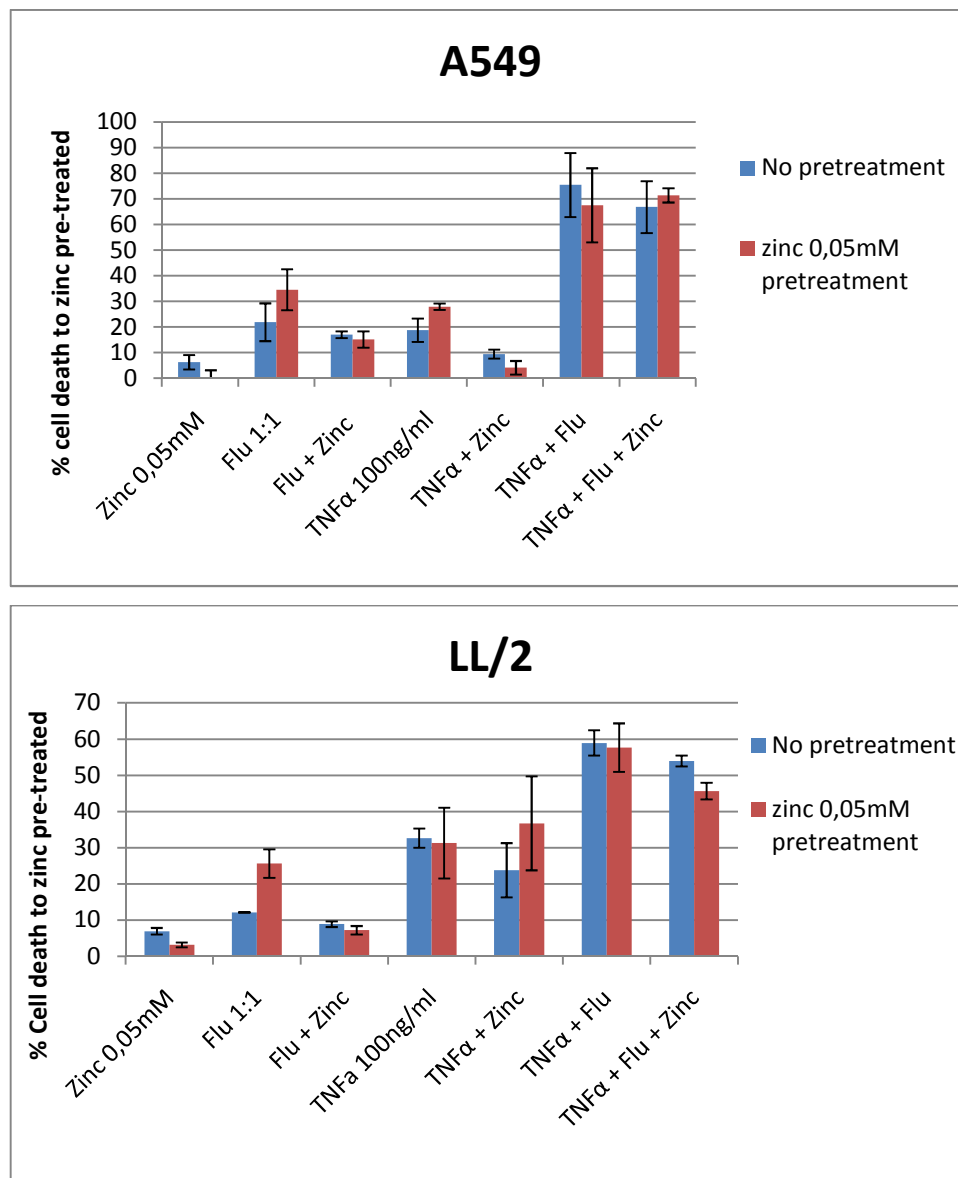
Figure 15: The cell lines LL/2 and A549 were either pre-treated with zinc or at the same time as the IAV infection. Zinc was removed from the pre-treated cells when IAV infection took place and only re added to rows indicated to have zinc. Pre-treatment led to a general higher cell survival. Depletion of zinc induced higher cell death in IAV infected and with the A549 in TNFα as well. No significant reduction of the synergistic effect from TNFα in combination with IAV can be observed. Data is representative of two independent experiments with three replicates in each group.

4 Project 2 – Influenza induced phagocytic defect in macrophages

4.1 Introduction

As already mentioned in 1.1, Influenza A virus induces an apoptotic cell death. Those dying cells then form apoptotic bodies, present molecules like phosphatidylserine on their cell surface and release chemo attractants (35; 49). These signals lead to the recruitment of macrophages to the lung which leads to a clearance of the apoptotic bodies by the macrophages (34). If these apoptotic bodies do not get cleared, they would turn secondary necrotic, leading to the release of pro inflammatory cytokines (35). Influenza, being able to infect alveolar macrophages as well as recruited monocytes/macrophages (2; 34), might have the potency to impair phagocytosis of these cells by macrophages. This would result in an inflammatory storm caused by secondary necrosis that is even further increased by coinfections.

Comparing uninfected with infected macrophages for their phagocytic ability was done at first by a double stain experiment. Seeing a reduction in the uptake of the infected macrophages we used a 3rd stain to label dead macrophages. Therefore we could be sure that only alive infected macrophages were compared to uninfected macrophages in their ability to phagocytose dead cells.

4.2 Results

4.2.1 Determining the right timing and amount of infecting macrophages with Influenza A Virus (IAV)

To have an optimal infection during our phagocytosis experiments the amount of cell death induced by IAV was determined (Figure 16). The first ratio of influenza virus to macrophages used therefore was 1:3 for 20 hours. After our results became inconsistent with this ratio of infection, we realized that we had been using less macrophages than expected. The mistake simply happened by not counting the macrophages after they had been stained. During the staining process a lot of cells died and the actual numbers of seeded out macrophages were therefore lower than first calculated. In the end we found out that due to this mistake we had been using a ratio of 2:1 influenza virus for 20 hours instead. Finally we decided to use the 1:3 as well as the 2:1 ratio of influenza infection over 20h for further experiments and compare the outcome to each other.
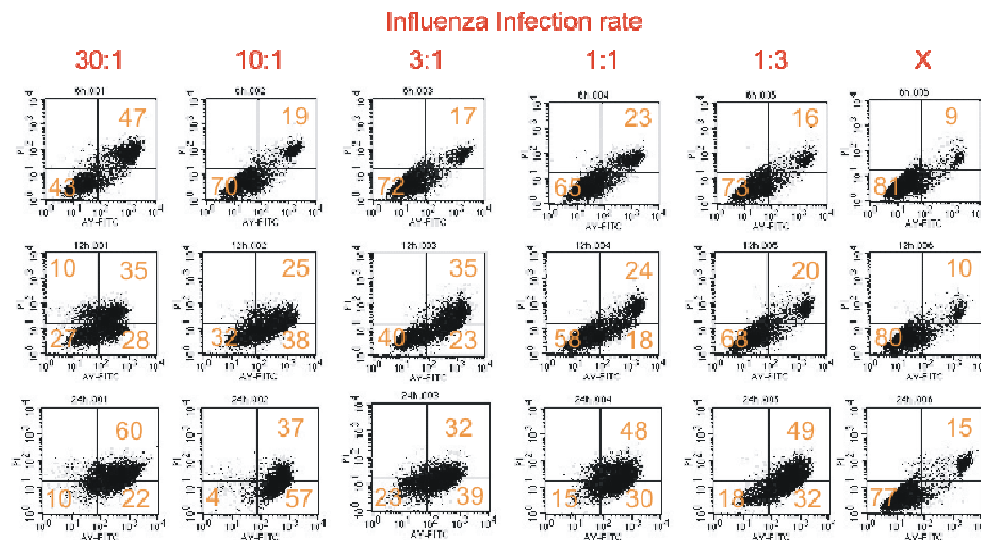
Figure 16: Determining the ideal ratio of IAV to macrophage to use for further phagocytosis experiments. Each square shows in the lower left: the percent of living cells; lower right: the percent of dying cells presenting Annexin V; top left: dead cells only labelled with PI; top right: dead cells double labelled with Annexin V and PI. The orange numbers represent the percentage of cells in that area. Top row measured after 6h, middle row measured after 12h, bottom row measured after 24h.

4.2.2 Influenza induced phagocytic defect in macrophages

As mentioned in 4.1, one reason for the immense lung epithelial damage and the following immunopathology seen in coinfected mice, might be the inability of the macrophages to take up apoptotic bodies that then turn secondary necrotic. IAV might be inhibiting a phagocytosis pathway. A ratio of 2:1 influenza virus was used to compare infected and uninfected macrophages in their ability to take up IAV, etoposide or untreated LL/2 cells. The LL/2 cells were put together with the macrophages over 1 hour, 2

hours and 4 hours. The results that we received led us to the conclusion that indeed an IAV infection seems to induce a defect in uptake (Figure 187, Figure 18).
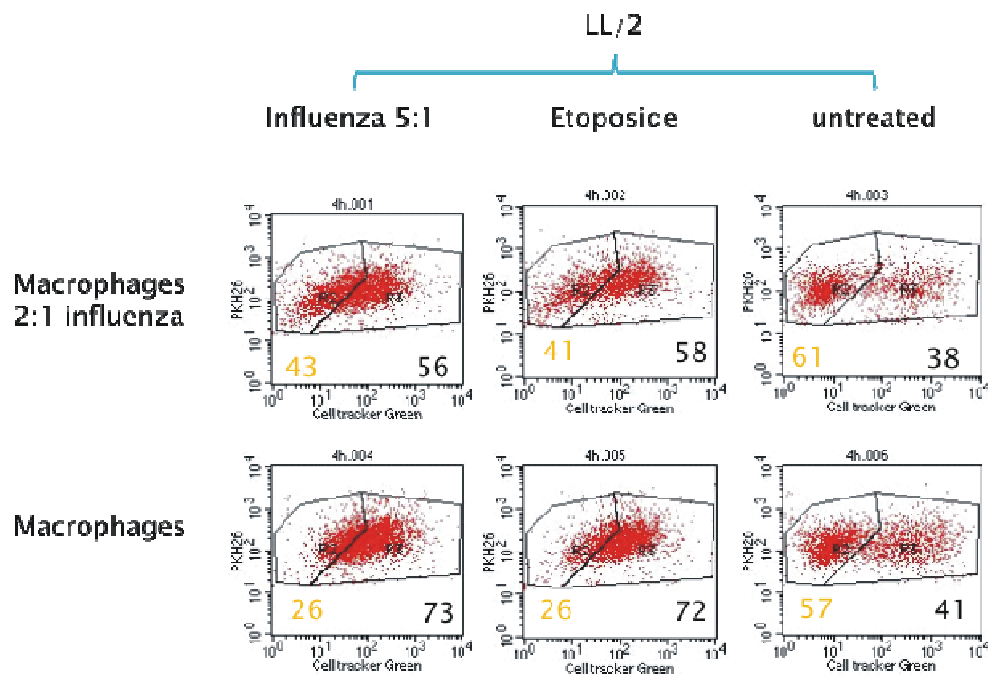
Figure 17: Example of a flow cytometry experiment. Showing a 4 hour combination of 5:1 influenza infected, etoposide treated or untreated LL/2 cells (from left to right lane) with either 2:1 infected (top row) or uninfected macrophages (bottom row). Yellow numbers represent the percent of macrophages that are single stained and therefore did not take up LL/2 cells. Black numbers represent macrophages that are double stained and therefore have taken up LL/2 cells. LL/2 cells were stained with cell tracker green. Macrophages were stained with PKH26.

Figure 18: 2:1 influenza Infected and uninfected macrophages are checked for their ability of phagocytic uptake from etoposide treated (top picture) and IAV infected LL/2 cells (bottom picture). The LL/2 cells were 1 hour, 2 hours or 4 hours combined with macrophages before getting analysed. Data is representative of one experiment with one sample in each group.
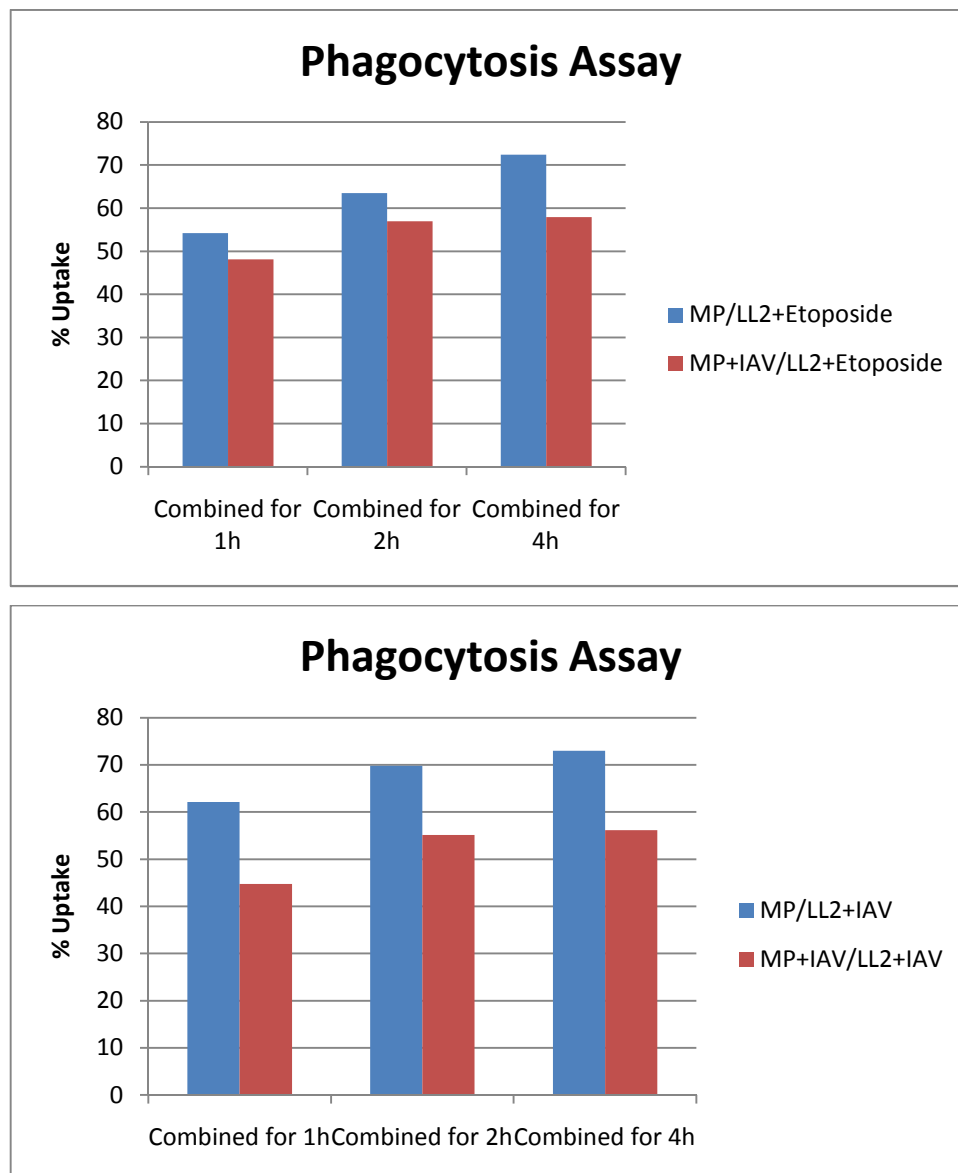
4.2.2.1 *Phagocytosis assay of living infected macrophages*

In our experiment around 60 percent of the influenza infected macrophages die and are therefore not able to take up any LL/2 cells. Dying macrophages will still be labelled with PKH26 and will be counted as macrophages that have not taken up anything. This might cause the difference in uptake between the infected macrophages and the uninfected ones. Gating only on our PKH26 labelled living cells (Figure 19) then showed us that the results stayed consistent in 4 independent experiments (Figure 20). The use of a 1:3 ratio of virus to macrophages showed us an opposite result. This indicated that the experiment is very sensitive an efficient IAV infection of the macrophages is essential for inducing the phagocytic defect (Figure 21). With the lower infection dose a higher uptake of LL/2 cells in the infected macropahges could be observed.
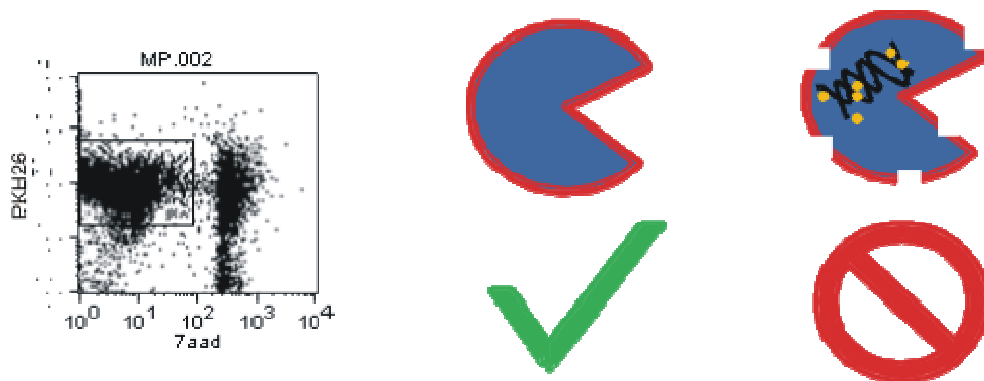
Figure 19: Flow cytometry setup for gating (left) on PKH26 labeled living macrophages (middle). 7aad staining only occurs if cell membrane is breached and 7aad can intercalate with the DNA (right). This only happens to dead cells and they are therefore differently labeled than living ones.
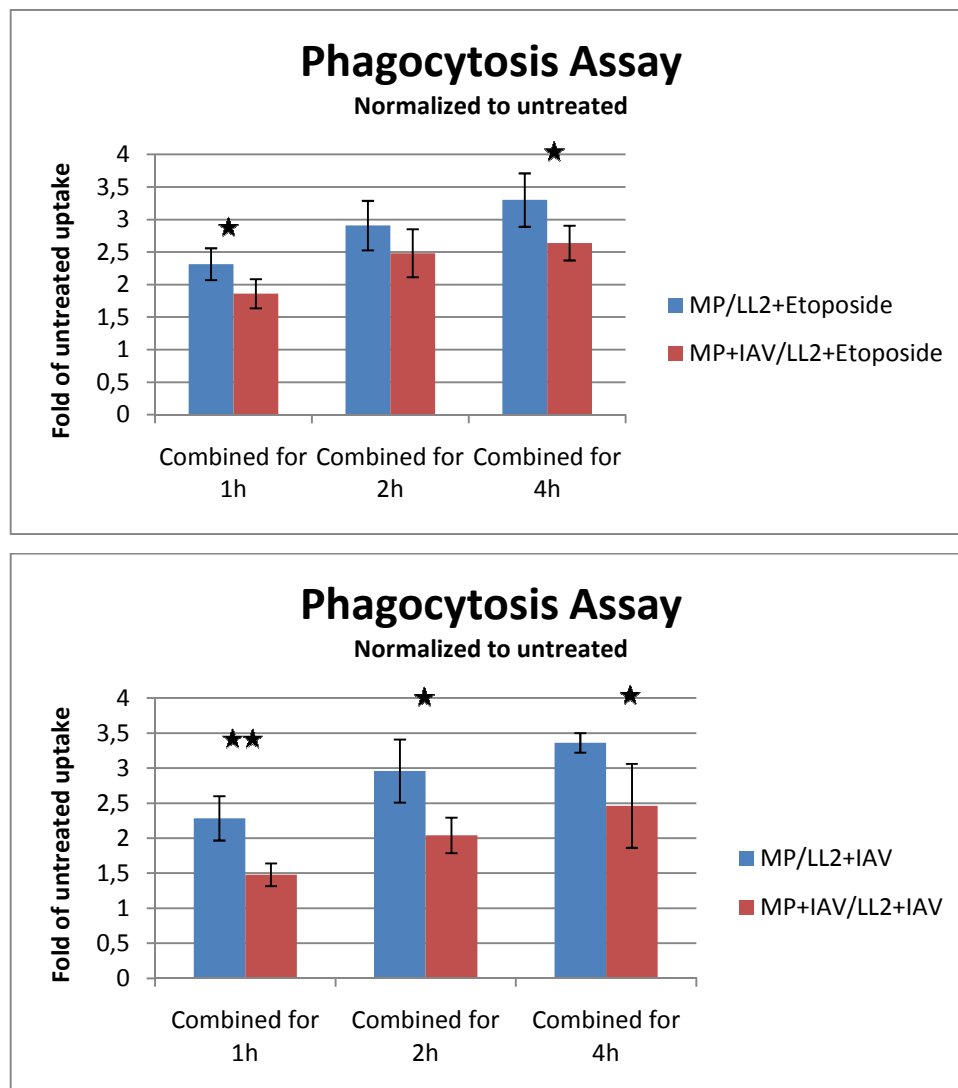
Figure 20: Only alive 2:1 infected and uninfected macrophages were checked for their ability of phagocytic uptake from etoposide treated (top picture) and IAV infected LL/2 cells (bottom picture). The LL/2 cells were 1 hour, 2 hours or 4 hours combined with macrophages before getting analysed. Data represents 4 independent experiments normalized to untreated LL/2 cell uptake due to varying background uptake. Data is representative of four independent experiments with one sample in each group. ** p < 0,01; * P < 0,05

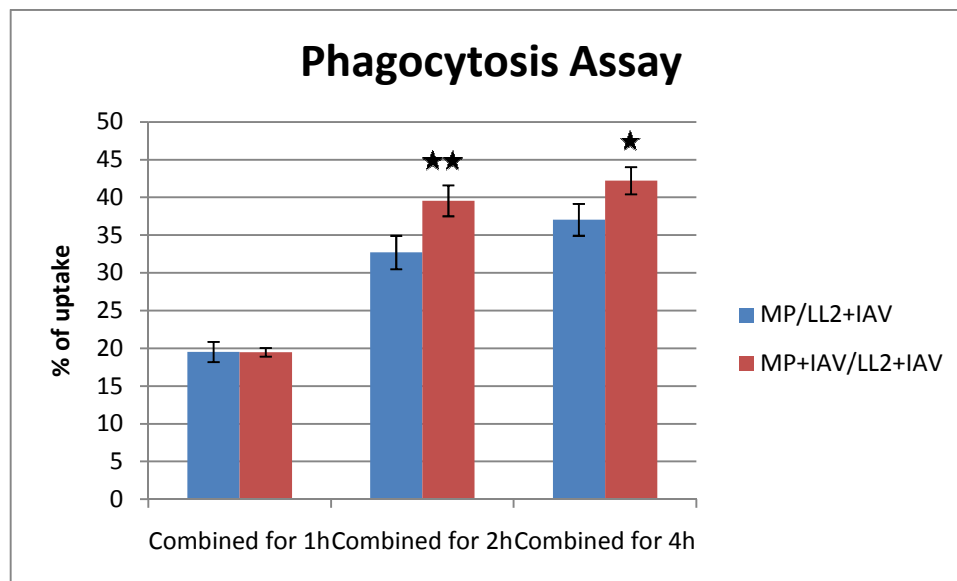**Figure 21:** Only alive 1:3 infected and uninfected macrophages were checked for their ability of phagocytic uptake. The LL/2 cells were 1 hour, 2 hours or 4 hours combined with macrophages before getting analysed. Experiment was done in a triplicate setup. Data is representative of one experiment with three replicates in each group. ** p < 0,01; * P < 0,05

5 Project 3 – Macrophage motility

5.1 Introduction

During a lung infection with influenza, the clearance of the virus by macrophages is essential. The available macrophages in the lung would not be sufficient to counter the infection. Therefore more macrophages have to be recruited. The migration into the infected tissue is directed by chemokines (14; 50) that are released during a common immune response as described in 1.2. The binding of the chemokines to cell surface receptors of the macrophages, activate signalling cascades that lead to the activation of Phosphoinositide 3-kinase (PI3K). PI3K then leads to the production of Phosphatidylinositol (3,4,5)-trisphosphate (PIP3). This is essential for the formation of actin filaments that direct the movement of the macrophages by forming filopodia.

As influenza virus is known to interact with PI3K (51), we wanted to analyze how infected macrophages would act differently in their motility compared to uninfected macrophages. Our live imaging experiments showed us that infected macrophages possibly release chemokines into the surroundings, as they are able to change the movement pattern of uninfected macrophage. We were also able to see a reduction of the movement speed of infected macrophages compared to uninfected Macrophages.

5.2 Results

5.2.1 Macrophage motility

Macrophages are essential in the immune response to influenza. Therefore we were interested in studying how infected macrophages changed their motility after infection. Surface staining of the viral M2 protein showed that all the macrophages were infected (Figure 22). By analysing their movement over 18h we could clearly see that the colony of infected macrophages did not spread far from the starting point, while uninfected macrophages spread out from the initial colony (Figure 23; Figure 24; Figure 25).
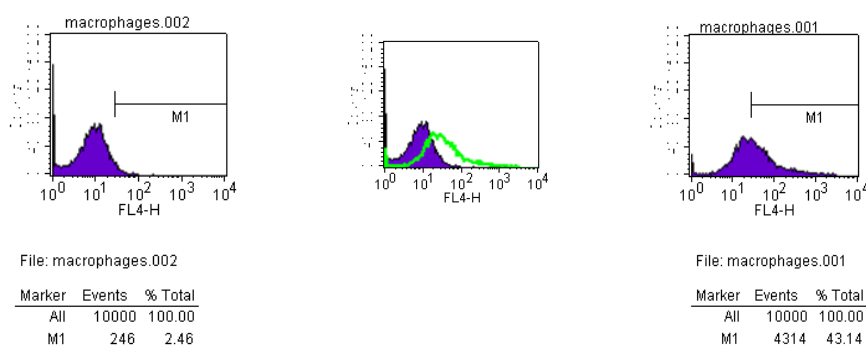
Figure 22: Uninfected macrophages (left) and infected macrophages (right) compared for the presentation of the viral M2 cell surface protein. An overlay (middle) shows a clear shift of the whole peak to the right for the infected macrophages (green line).
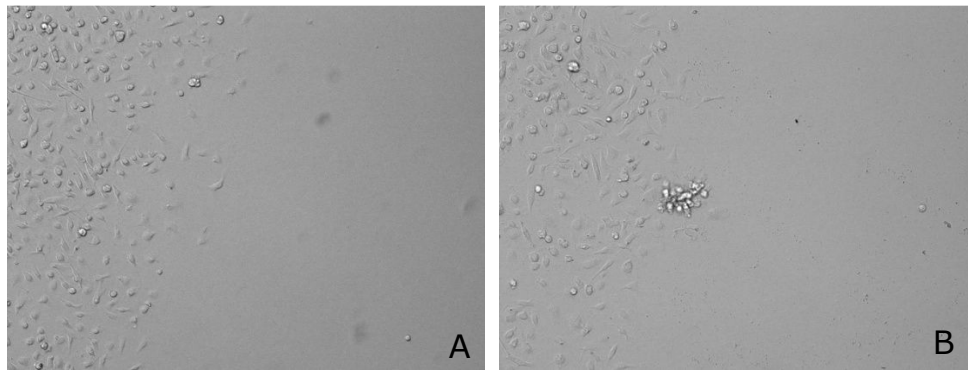
Figure 23: Uninfected macrophages (A) and infected macrophages (B) at **0h** of the live imaging analyses. Data are from one live imaging experiment.
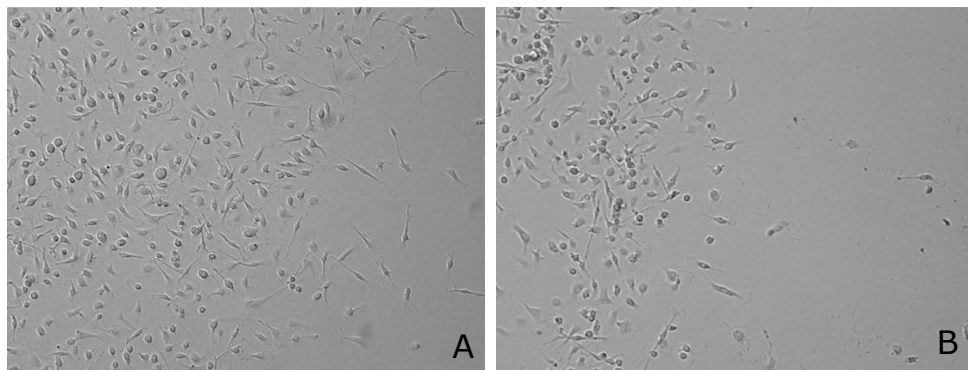
Figure 24: Uninfected macrophages (A) and infected macrophages (B) at **8h** of the live imaging analyses. Data are from one live imaging experiment.
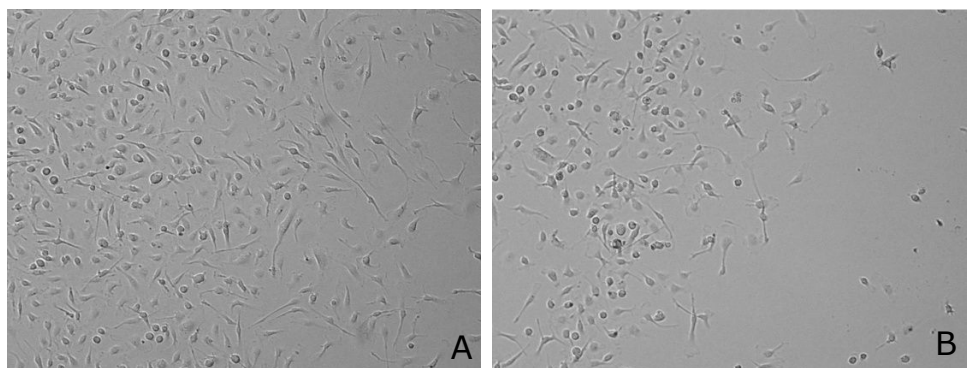
Figure 25: Uninfected macrophages (A) and infected macrophages (B) at **18h** of the live imaging analyses. Data are from one live imaging experiment.

5.2.2 Influence of infected macrophages on uninfected macrophages motility

To check if the movement deformation was directed by the infection, PKH26 labeled uninfected macrophages were put together with unlabeled infected macrophages in one colony. Live imaging over 18h showed us that uninfected macrophages acted like infected macrophages (Figure 26). No difference in the spreading could be observed.
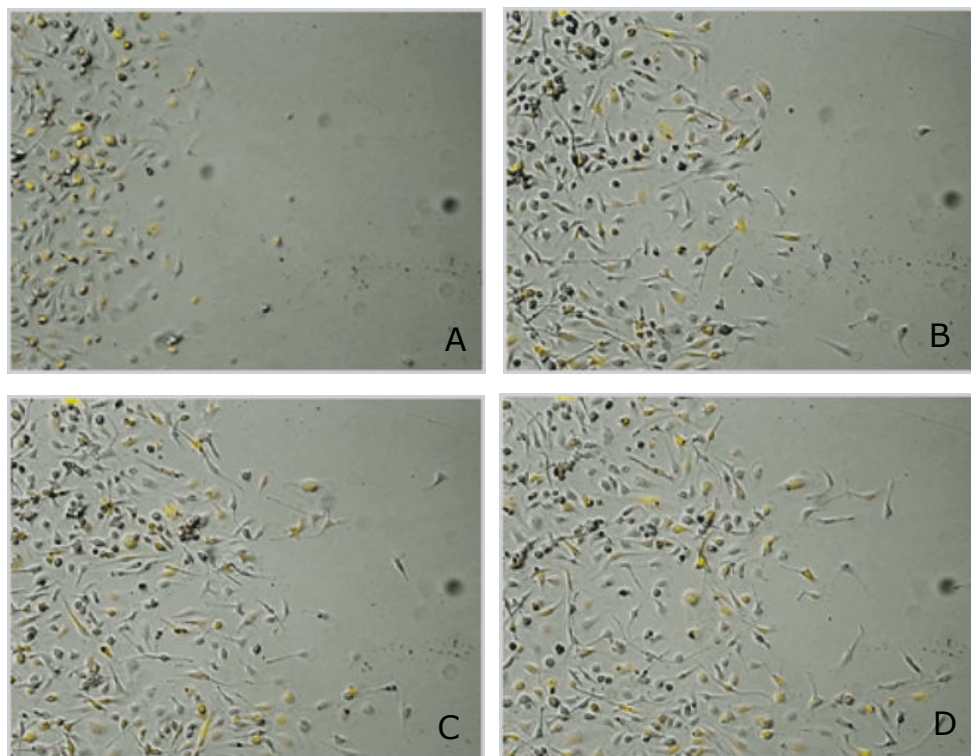
Figure 26: PKH26 uninfected macrophages (yellow) and infected macrophages (transmission) compare to each other in one colony over 18h. Pictures show 0h (A), 6h (B), 12h (C) and 18h (D) time points. Data are from one live imaging experiment.

5.2.3 Differences in speed of infected macrophages compared to uninfected macrophages

The next step was to see if there is a difference in the actual movement speed of macrophages during a colony spread. We therefore took shorter time intervals to be able to follow the macrophages from one picture to the next one. There was an observable difference between the uninfected and infected macrophages. Infected macrophages were around 25µm/h slower than uninfected macrophages (Figure 27).
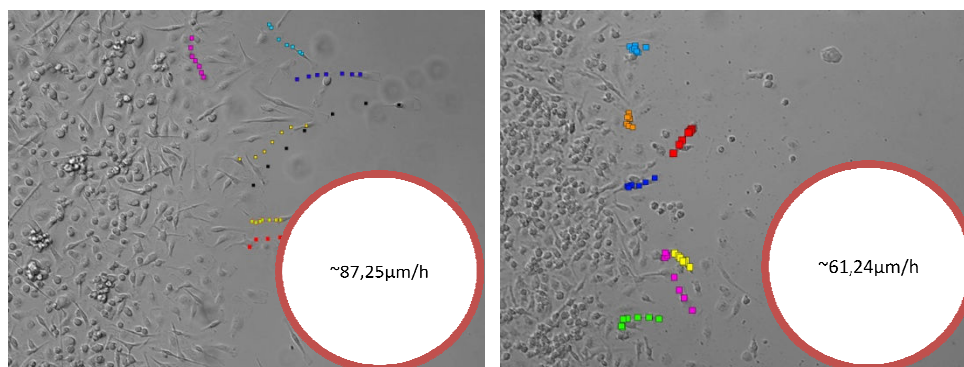
Figure 27: Speed measurement of uninfected macrophages (left) and infected macrophages (right). Colored squares indicate the movements of one macrophage over a time period of 1h, placing one square every 10min. 7 macrophages were manually followed to receive the data. Data are from one live imaging experiment.

Again also the movement direction showed a more even spreading movement away from the colony by the uninfected macrophages. Infected macrophages in comparison were generally zigzagging on one spot and stayed close to the colony.

6 Discussion

Coinfections are very complex and manifest differently between different types of pathogens. Therefore we have not covered all mechanisms and possibilities involved during these infections. Our results though are the first step of putting the pieces of the Influenza A virus and *L. pneumophila* coinfection puzzle together.

We showed a synergistic effect on cell death in our lung epithelial cell lines between TNFα and IAV infected cells (Figure 6, Figure 7). Showing that this effect is only visible if the TNFα is added 5h after the infection of the virus (Figure 11), demonstrates that viral infection alters the intracellular machinery in some way, that the addition of TNFα then causes the cell to follow an apoptotic pathway. One reason for the enhanced cell death could be the expression of type 1 Interferons (IFN-α/β), which as mentioned under 1.2, act to form an antiviral state (14) and are known to prime macrophages to become susceptible to further apoptosis or necrosis (52; 53). Knowing what the different influenza viral proteins are able to do, (9-11; 54) we cannot exclude a possible correlation between one or more yet unknown functions of the viral proteins and in that case a direct transformation of the TNFα pathways. Already other bacterial and viral strategies have been identified to manipulate the TNFα induced pathways (38) (Figure 28). Influenza might regulate the NF-κB pathway and in that

case TNFα would not be able to induce the production of survival signals but would only be able to induce cell death. Another possibility would be the viral NS1 protein which is able to regulate cell survival. First it blocks apoptotic pathways by inhibiting p53 and after replication and spread of new virus it induces cell death (9). TNFα stimulates accumulation of p53 (55), which in that case might overcome the regulation by the NS1 protein. This would lead to an increased cell death of the viral infected cells. It could be though that influenza is not regulating the pathways that lead to apoptosis by TNFα. It might rather try to inhibit their activation by blocking the translation of TNFα. There is a study that proposes that TNFα mRNA gets highly produced after influenza infection but only is released efficiently as a protein after lipopolysaccharide (LPS) stimulation (56). Already highly stressed cells having to deal with higher levels of TNFα, might then push them into an apoptotic pathway. Therefore these higher levels of TNFα during coinfections (31) compared to a viral infection alone might be an answer.
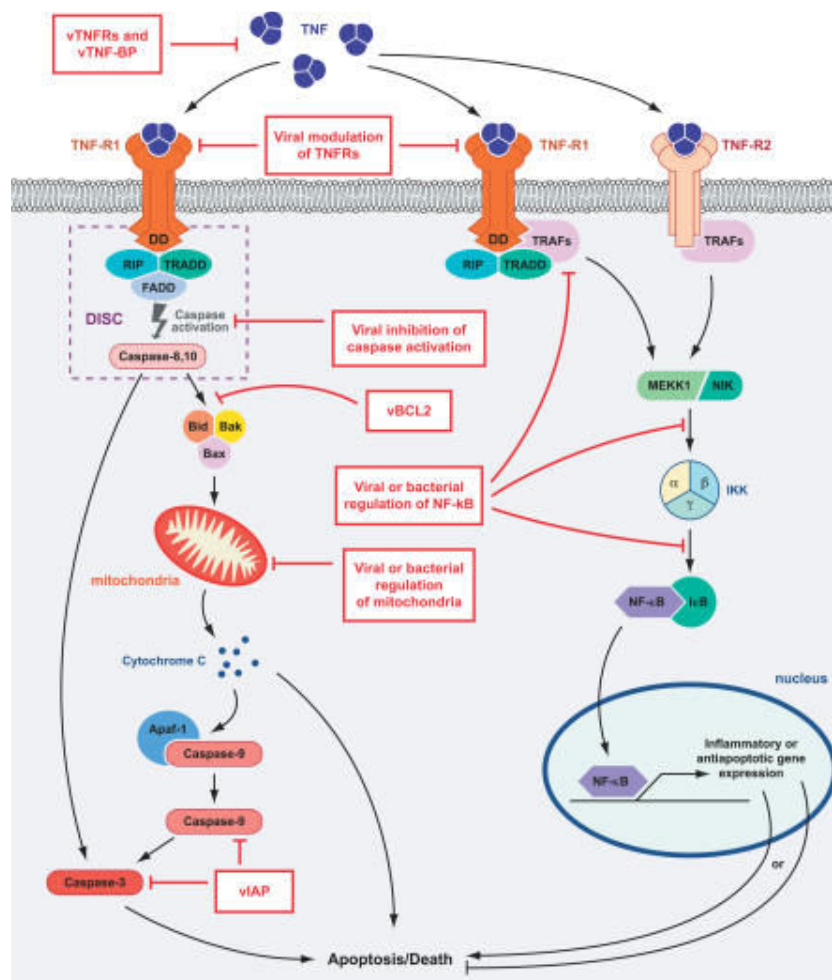
Figure 28: Showing different strategies of viral and bacterial proteins to influence TNFα induced pathways **(38)**.

Source: Rahman MM, McFadden G. *Modulation of Tumor Necrosis Factor by Microbial Pathogens*. PLoS Pathog 2006 Feb;2[2]

The results that we received from our primary cells were inconsistent. Having both a synergistic effect similar to the cell line data (Figure 14) but on the other hand having a rescue effect by TNFα (Figure 13). The difference between the experiments was obviously the well size as we once used a 96-well plate and once a 24-well plate. The cell density might be the key difference between the

experiments and what cell density corresponds to the lung environment is an important question to address. This has to be checked in further experiments.

We next examined if we can rescue the cells from this synergistic effect that we saw with our cell lines. Finding a way to counteract *in vitro* against the deadly effect of TNFα, would give us a chance to try and enhance the survival of coinfected mice *in vivo*. We therefore tried zinc, which as mentioned in 3.1 is a cytoprotectant and anti apoptotic agent (32; 33). It interacts directly with caspase-3 which is one of the targets to be activated by IAV and TNFα. (44; 43). The different approaches of either pre-treating our cells with zinc or adding zinc at the same time, as the infection took place, did not show us a rescue against the synergistic effect (Figure 15). However, if the zinc was removed from the cells after pretreatment, they were indeed more susceptible to IAV & TNFα induced cell death. This could be one of the things happening *in vivo*, as during bacterial infections the zinc levels get reduced (40).

Trying different timings of when zinc is added could give us more relevant information for a possible role of zinc. For example we could try to culture the cells in zinc supplemented medium for a week. This might change the intracellular response to pathogens even further than just pre-treating them for one night. The depletion of zinc could in that case show us an even stronger negative effect. The depletion of zinc 5 hours after IAV infection, when TNFα is added, would also be very interesting to see. This would

reflect even better what we are able to see during coinfections. Further it might cause an even more drastic difference compared to cells where the depletion was counteracted by addition of more zinc. The last approach could be by looking at the *in vivo* situation by giving mice a zinc supplemented diet and look at the death rate of the mice after coinfections.

All our experiments were done *in vitro* which is much different than the *in vivo* situation. The cells were without a functional immune system and had no real way to counter the viral onslaught. So we were not able to know if TNFα is the only key element in the immunopathology that is going on *in vivo*. *In vivo* experiments done in TNFα knockout mice by Amanda M. Jamieson (unpublished data), showed the single infected mice did not have any defect in their capability of surviving a sublethal dose. The coinfected did not show an increase in survival and all mice died at the same time as wildtype mice (Figure 29). However, it is clear that the synergism between IAV and TNFα exists *in vitro* and may contribute in some way to the deadly outcome of coinfected mice. However, other factors also appear to play a role during an actual coinfection.
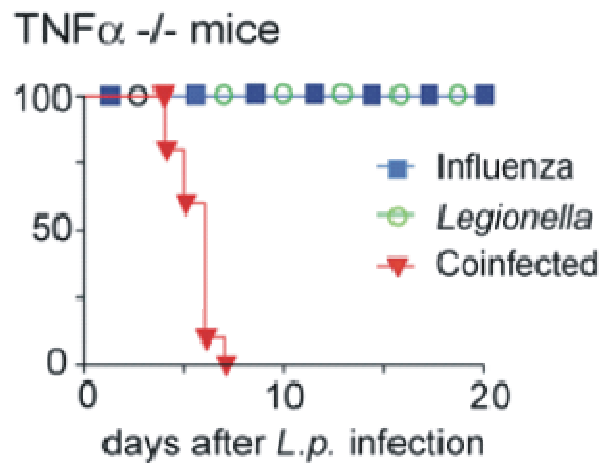
Figure 29: TNFα knockout mice treated by sub lethal doses of Influenza, Legionella and coinfection. (unpublished data by Amanda M. Jamieson)

One of these factors for the increased lung damage seen in coinfected animals could be the decreased phagocytosis of dead and dying cells by infected macrophages. Our experiments focused directly on the infected macrophages and compared their phagocytic ability with uninfected macrophages. The data suggest that *in vitro* an IAV infection has a direct impact on the functionality of live macrophages. This is manifested not only in a reduction of uptake of apoptotic cells, both IAV infected and etoposide treated (Figure 20), but also in an altered motility (Figure 23 – 25, 27) compared to uninfected macrophages. Keeping in mind that only a high dose of IAV led to a reduction of uptake (Figure 20), while lower doses of IAV led to an actual increase in the phagocytic ability of infected macrophages (Figure 21), the possibility of an artificial result of this very

sensitive experiment cannot be excluded. However, the possibility remains that only an efficient infection of the macrophages leads to an inhibition of the phagocytic ability, which was only seen with the higher dose of IAV. But as neither *in vitro* primary cell, nor *in vivo* experiments have yet been executed from our side to provide us with more in depth information of the actual happenings, further examinations have to be made. This is important as BMDM might have different ways to react to an IAV infection than would normal alveolar macrophages (AM). In addition, using primary lung epithelial cells, which also might act different than tumor cell lines, may allow us to look at a more physiological response.

What has not been addressed in this diploma thesis but would also be interesting to look at is if infected macrophages have reduced numbers or completely missing cell surface receptors, which would be needed to bind and take up dead cells. The removal of these receptors could be accomplished by the viral NA which, as mentioned in 1.1, is known to be responsible for cutting sialic acids on the cell surface to bud off.

The last thing that caught our attention was IL-10, which is known to suppress TNFα expression and also enhance the phagocytic ability of macrophages (57; 58). Final results showed us that infected macrophages seem to express less IL-10 compared to uninfected macrophages (data not shown). To check for the actual mRNA level of IL-10 will be the first step here. This might already show differences to the measured supernatant. From there it will

be immensely interesting to see if the reduction of IL-10 proves to be true *in vivo* as well. If this would be the case, then this could be a reason for a reduction of the phagocytosis that we have seen. Further it might give us an idea of why we see an immunopathology that with a normal expression of IL-10 might not happen.

Clear results came from the movement of the infected macrophages. Uninfected macrophages had a directed movement away from the colony, while IAV infected macrophages stayed close to the colony and had a reduced spreading movement. We then examined if this effect was cell autonomous. It might also be that this pattern is induced through to release of chemokines, as mentioned in 1.2, which would influence the movement of uninfected macrophages if presented to them. Combining uninfected macrophages with infected macrophages in the same colony, led to an adjustment of the uninfected macrophages to the infected macrophages. Both movement patterns became the same (Figure 26). Our first thought of chemotaxis directed movement seemed to be reasonable.

Future experiments should give us more insight into the possible mechanisms for this phenomenon. Optimizing the colony spreading experiment would be the first step here. This could be done by looking at the whole colony while it is spreading, instead of looking only at a small fraction of the colony. Next thing would be to use chemo attractants or the supernatants of infected macrophages. They would be added to uninfected macrophages. If their

movement pattern would change, this could prove that chemokines are responsible for the alteration in the movement of the macrophages. During infections this would lead to a macrophage infiltrate into the infected region. The production of further chemokines would therefore attract even more macrophages. This high number of macrophages would be necessary to clear the infection. Higher amounts of macrophages also means higher amounts of inflammatory cytokines produced and this might be one of the reasons for the immunopathology that we see.

In addition to the observable difference in the type of movement, the actual speed of the macrophages proved to also be interesting. The difference that could be seen not only showed us a reduction of over one quarter of the uninfected macrophage speed but also again a zigzagging movement pattern by the infected macrophages, compared to a more outward bound movement by the uninfected macrophages (Figure 27). There are several possibilities for these observed differences that will require further research to confirm. During our experiments we were able to observe that infected cells are generally more adherent than uninfected ones, one of the reasons could be that one of the viral proteins leads to an increased adherence of the macrophages, which makes it harder for them to move on. Another possibility and simple answer could be that the macrophages are already close to death and therefore have a highly reduced motility. This though can most likely be excluded as we only looked at macrophages which still showed their filopodia and therefore were alive. An

additional 7-aad staining would make it easier to only count living macrophages. For more accurate results of the speed measurement, a computer tracking software which is able to track every single cell over an even longer period of time, would be needed.

If we look at the big picture now, we can say that one mechanism alone is not capable of leading to the immunopathology that we see *in vivo*. In fact it is very likely that all the mechanisms are linked to each other. First we have an influenza infection in the lung. The immune response leads to the production of chemokines, attracting macrophages to the site of inflammation (Project 3). There the macrophages get infected and therefore are weakened in their ability to phagocytose dead cells (Project 2). Under normal circumstances, they would still be able to handle the infection. During coinfections this is different. Once the bacterial infection takes place, it triggers the higher release of TNFα. The combination of viral infection and TNFα leads to a higher cell death (Project 1). This is too much to phagocytose for the infected macrophages, leading to the release of pro-inflammaory cytokines and subsequently to immunopathology. Unraveling more interactions during coinfection, which are linked to the ones we have identified, will be very interesting in the future.

7 Materials and Methods

7.1 Mice

C57BL/6 (B6) mice were obtained from Charles River. They were between 6 and 10 weeks old.

7.1.1 Bone marrow derived macrophages (BMDM)

The BMDM were taken from the tibia and the femur of B6 mice and cultured in DMEM (PAA) supplemented with 10% FCS (Sigma), 10% L.condition, Penicillin and Streptamycin (Invitrogen) in 100mm square Petri dishes (Sterilin). Supernatant from L929 cells was a source of colony stimulating factor-1 (CSF-1) used to grow BMDM. (59).

The cells were fed after day 3 with 5ml medium. On day 5-7 they were scraped off and split into three times the amount of dishes. Between days 10-18 the BMDM were seeded out for further experiments.

1000x Pen/Strep: 0,06%   Penicillin

0,1% Streptamycin

Dissolved in 1ml H_2O

10x PBS: 81mM $Na_2HPO_4.2H_2O$

                            15mM KH_2PO_4

                            25mM KCl

                            1,4M NaCl

                            pH = 7,4

7.1.2 Primary Lung epithelial isolation (46)

On the day before the isolation of the lungs a 100mm tissue-culture-treated Petri dish (Nunc) was coated with 50µg of CD45 rat anti-mouse Antibody (Becton Dickins) and 40µg of CD16/32 anti-mouse Antibody (Becton Dickins) in 5ml PBS. Additionally untreated cell culture plates or chambers (Nunc) were coated with Collagen IV (Sigma) at a concentration 1µg/ml. Both plates were then sealed with either fresh keeping foil or parafilm and placed at 4°C over night. Directly before their use, the plates were washed 2 times with PBS.

To avoid disturbing the trachea mice were euthanize with CO_2. Using a dissection board the 70% ethanol cleaned mouse was cut open at the peritoneum. From there the diaphragm was cut out carefully to not injure the lungs. The sides of the ribcage were cut to ensure a good access to the heart. Fat was removed from around the heart and a cut was executed at the vena cava, which can be found at the

top left part of the heart. This is to prevent any backflow from flushing the heart. The right chamber of the heart was now invaded with a 0,8mm needle to perfuse the lung, thus clearing them of blood cells, with 20ml NaCl. Now the airway was exposed and after removing additional tissue, a hole was cut into the trachea. A piece of suture thread was wrapped around the airway and pulled tight after inserting 3ml Dispase I with a flexible silicon tube (Helixmark) connected to a syringe, to avoid the backflow of the Dispase I. Through the same silicon tube, 0,45ml of the LMP agarose was very carefully inserted, to not mix it with the Dispase. Ice was then used for 2 mins to polymerize the LMP agarose. The lung was cut out and placed in 1ml Dispase for 45min at room temperature. After that time, it was placed on ice until further use.

The lung was taken out into a 100mm Petri-dish with 7ml of DMEM + 0,01% DNase I and 2 bent forceps were used to rip the lung into tiny pieces. The cell isolate was taken up with a 10ml syringe and filtered two times through 70µm mesh filter (Becton Dickins), mashing it through with the back side of a 2,5ml syringe. The cells were then centrifuged at 130g for 12min at 4^oC. After that the supernatant was taken off and the pellet was resuspended in 10ml DMEM + 10% FCS. The cell suspension was then poured into the CD 16/32/45 coated Petri-dish and incubated at 37^oC for 2 hours.

The supernatant was collected and 1ml was used to determine the total cells via Vi-Cell, Cell viability Analyzer (Beckman Coulter). After that the cells were centrifuged at

130g for 12min at 4°C. They were then taken up in Ham´s
F12 medium in a concentration of 1.10^5 cells/ml. Now either
1ml/well was added to a 24 well plate or 100µl/well to a non
collagen coated 96 well plate.

The next day the medium and all non adherent cells
were sucked off and fresh Ham´s F12 medium was added
for optimal conditions. This was repeated 2 times, with 3
days in between, until further experiments were started.

0,9% NaCl: 0,9g   NaCl
                              100ml ddH$_2$O
                              Sterile filtered

1% low melting agerose: 1g Low melting point (LMP)
                              agarose
                              100ml ddH$_2$O
                              Autoclaved
                              20 minutes before use keep at
                              37°C water bath

Dispase I (Sigma):   2mg   Dispase I
                              20ml PBS
                              Sterile filtered
                              Kept 5ml aliquots at -20°C

DMEM + 0,01% DNase I (Sigma): 10mg DNase I
                                       100ml   DMEM
                                       Sterile filtered

DMEM + 10% FCS: 500ml DMEM

                            50ml FCS

                            500µl Pen/strep

Ham´s F12 medium: 15mM   Hepes

                            0,8mM $CaCl_2.2H_2O$

                            0,25%   Bovine   Serum
                            Albumin (BSA)

                            Used I1884 Sigma:

                            5µg/ml   Insulin

                            5µg/ml   Trsansferring

                            5ng/ml   Sodium selinite

                            10%   FCS

                            pH = 7,4

                            Sterile filtered

7.1.2.1 Staining for primary Lung epithelial cells (LECs)

Lab-Tek 4 Well Permanox Chamber slides (Nunc) were coated with 500µl Collagen IV (Sigma) at a concentration of 1µg/ml. Before further use the chambers were washed 2 times with 1ml PBS. Taken up in Ham´s F12 medium, 1.10^5 cells were added to each chamber.

The next day the medium and all non adherent cells were sucked off and fresh Ham´s F12 medium was added

for optimal conditions. This was repeated 2 times with 3 days in between.

On day 7 the chambers were washed 2 times with PBS. Afterwards the cells were fixed using 1ml 3% PBS/PFA (Paraformaldehyd) for 10min. The cells were washed 2 times with 1ml PBS and then 0,1% Triton was added to permeabalize the cell membrane for the antibody (AB). The cells were again washed 2 times with 1ml PBS and then blocked for 1h using 5% milk.

After blocking, the cells were washed 2 times with 1ml PBS. The primary AB, purified mouse anti-E-cadherin (Becton Dickinson), was added in 300µl of 3% BSA with a concentration of 5µg/ml (1:50 dilution) to the first 2 chambers. The second 2 chambers received only 300µl of the 3% BSA as controls. The chamber slide was wrapped in parafilm and placed on a slow shaker on 4°C over night.

On the next day the chamber slide was washed 2 times with 1ml PBS for 5 minutes. The secondary AB, chicken anti-mouse AB alexa fluor 488 (Becton Dickinson), was added in 1ml of 5% milk with a concentration of 4µg/ml (1:500 dilution) to the first 3 chambers. The last chamber only received 1ml of 5% milk. The incubation was done at RT in the dark for 1h.

The cells were washed 2 times with 1ml PBS for 5 minutes and then stained with 1ml of a concentration of 0,3µg/ml (1:3000 dilution) DAPI diluted in PBS. The incubation was done at RT in the dark for 10min. The cells were washed once more with 1ml PBS. Immediately afterwards the construct on top of the slide was ripped off

and 2 drops of darko fluorescent mounting medium (Dako) was added onto each chamber area. Very carefully a 24 x 50mm cover slip was lowered onto the slide, pushing all air out of the area.

The slide was then placed at RT in the dark over night to let the mounting medium harden. Once hardened the slide was looked at with the Olympus Cell-R Live Imaging Unit (Olympus) with an amplification of 10.
After use the slide was kept at 4°C in the dark.

5% milk:	0,25g milk powder
	5ml PBS
3% BSA:	3g BSA
	100ml PBS
	Sterile filtered
4% PBS/PFA:	4g paraformaldehyde
	100ml PBS
	Dissolve it under constant stirring
	Once dissolved keep at 4°C

7.2 Viral Strain

The A/WSN/33(H1N1) strain of influenza A virus was originally obtained from the laboratory of Dr. Akiko Iwasaki. (31)

7.2.1 Propagation of Virus (60)

MDCK cells were grown until they were confluent in a $75cm^2$ cell culture flask (Nunc). They were lifted off by Trypsin-EDTA (PAA) and taken up in 40ml medium. 2ml medium with cells was added to each well of three 6-well multidishes (Nunc). 4ml were used to keep MDCKs growing. On the next day the medium was aspirated off using autoclaved Pasteur pipettes. The wells were then infected with 200 PFU of virus in 100μl of DMEM with 1% BSA (MP Biomedicals). The 100μl were spread by shaking the dish and left on for 5-10 minutes. Another 1,5ml of DMEM+BSA was added and the dishes were left to incubate at 37^oC with 5% CO_2. After 48h the supernatant of each well was harvested and pooled into 50ml tube (Falcon). The cell debris was spun down by centrifuging at 2000rpm for 10min. The supernatant was removed to another 50ml tube and subsequently aliquoted into Cryo tubes (Nunc) that were frozen down at -80^oC.

7.2.2 Plaque Assay for WSN Influenza Virus

MDCK cells were grown until they were confluent in a $75cm^2$ cell culture flask (Nunc). They were lifted off by Trypsin-EDTA (PAA) and taken up in 40ml medium. 2ml medium with cells was added to each well of three 6-well multidishes (Nunc). 4ml was used to keep MDCKs growing. The virus was diluted into 1:10; $1:1.10^2$; $1:1.10^3$; $1:1.10^4$; $1:1.10^5$ concentration using PBS+BSA buffer. MDCK cells were washed once with PBS. Then each dish was infected with 100µl of each virus dilution and one well with PBS+BSA buffer as negative control. The cells were incubated for 1h at 37^oC with 5% CO_2. Every 10-15min the dishes were shaken to avoid drying. During incubation the overlaying mixture was prepared and, as well as the 2% low melting agerose, kept at 37^oC water bath at least 20min before further use.

After the incubation the virus was aspirated and the overlying mix was combined with the low melting agerose. 2ml of the mixture was added to each well immediately. The dishes were kept at room temperature with open lid for around 5min to let the agar solidify. The dishes were then incubated upside down for 2-3 days at 37^oC with 5% CO_2. After the incubation the plaques were counted to acquire the virus concentration.

100x Ca/Mg:	1,327mg $CaCl_2$
	2,133mg $MgCl_2$
	100ml H_2O

PBS+BSA: 0,315mg   BSA

                           1,5ml   100x Ca/Mg

                           148,5ml   1x PBS

                           Sterile filtered

2x DMEM+BSA: 12g DMEM powder

                           1,2mg NaHCO$_3$

                           2,1mg BSA

                           500ml ddH$_2$O

                           Sterile filtered

1% DEAE-dextran: 1mg DEAE-dextran

                           100ml ddH$_2$O

                           Sterile filtered

5% NaHCO$_3$:   5mg NaHCO$_3$

                           100ml ddH$_2$O

                           Sterile filtered

2% low melting agerose: 2mg low melting agerose

                           100ml ddH$_2$O

                           Autoclaved

Overlaying mixture: 25ml 2x DMEM+BSA

                           0,5ml 1% DEAE-dextran

                           1ml   5% NaHCO$_3$

                           25µl trypsin (Gibco)

                           0,5ml Pen/Strep

7.3 Cell lines

The cell lines A549 (carcinomic human alveolar basal epithelial cells), LL/2 (Lewis lung carcinoma passaged routinely in C57BL6 mice) and MDCK (Madin-Darby canine kidney) were cultured in DMEM (PAA) with 10% FCS (Sigma), Penicillin and Streptamycin (Invitrogen) in cell culture flasks (Nunc) of sizes between $25cm^2$ and $175cm^2$, dependent on the amount of cells needed for the experiments. They were split every 2-3 days using Trypsin-EDTA (PAA) to lift hem off.

The cell lines MLE12 (alveolar lung epithelial) and MLE15 (bronchial lung epithelial) were cultured in RPMI1640 supplemented with 2% FCS (Sigma), Penicillin and Streptamycin (Invitrogen), 2,5ml of Insulin, transferring and sodium selenite (Sigma I-1884), 250µl of Transferrin (Sigma T-1428), 50µl of Hydrocortisone (Sigma H-0888) and 50µl of b-Etradiol (Sigma E-2758) in cell culture treated 60mm Petri dishes (Falcon). They were split 1:5 every 3 days using PBS supplemented with 2mM EDTA (Sigma), added from a 500mM EDTA stock solution, to lift them off.

7.3.1 Mycoplasma test and treatment

Five ml of cell culture supernatant was taken up and centrifuged at 1500rpm for 5min. 500µl supernatant was taken and used for analyses with a luciferase assay (61). If cells were tested positive, they were treated with ciproxin in

a 1:500 dilution for 10 days. The antibiotics were changed every 2 days.

7.4 Freezing and thawing of cells

Cells were spun down with 1400 rpm for 5min and supernatant was removed. The cells were then taken up in 90% FCS and 10% DMSO. 1ml of the cell suspension was put per cryotube and placed at -80°C immediately. When cells are being used again they are thawed fast and mixed with their working medium to be placed in their incubator as normal.

7.5 Live imaging

The macrophages were counted with the Vi-Cell, Cell viability Analyzer (Beckman Coulter) and taken up in Macrophage medium (see 7.1.1), to have 1.10^{6} cells/ml. Imaging was done on uninfected and infected macrophages. Infected macrophages were incubated for 20h with 1:3 influenza virus before the live imaging was started.

Two pyrex cloning cylinders of the size of 6mm x 8mm (Sigma Aldrich) each were placed on a 35mm poly-d-lysine coated gamma irradiated glass bottom culture dish with 14mm glass and No. 1.5 glass thickness   (MatTek corportaion). Exactly 100µl, were then inserted into each of the cylinders, without touching or moving them. Having the front of the tip touch the glass ensured that no air bubbles

were formed and cells could spread evenly. Two– 2 ½ hours later a Pasteur pipette was used to suck off the medium and lift off the cloning cylinder, to not disturb the now formed colony. 2ml of fresh medium was inserted at the edge and distributed over the plate. The live imaging was done with the Olympus Cell-R live Imaging Unit with an amplification of x10. The cells were kept in an incubation chamber (40°C lid; 38°C bottom) with 5% CO_2. Pictures were made every 30min over time periods of 18h.

7.5.1 Measuring the speed with live imaging

The procedure for analyzing was mentioned in 7.5. Differences were: Infected macrophages were treated with 2:1 influenza virus before the live imaging was started. Pictures were made every 5min over a time period of 4h.

Coral Photo-Paint 12 was used to evaluate the speed. 7 pictures were placed over each other. The time window from one picture to the next was 10min. A square was drawn over the center of a macrophage in a certain color. Then the top picture was faded out and the next square was drawn over the new center of the macrophage. This was repeated for all 7 pictures. Only macrophages that formed filopodia were taken into account. The picture was then printed out and distances were measured with a ruler, taking the distance from the middle of one spare to the middle of the next square. Knowing the millimeter to

nanometer ratio the speed was calculated taking the mean of all measured macrophages.

7.6 LDH-Assay (45)

LDH is released from dead cells and can then be measured by adding Lactate which is oxidized to Pyruvate forming NADH. In addition with Tetrazolium salt, Formazan is being formed which then can be measured to estimate the cell death percentage.

7.6.1 Analysing cell death from IAV and/or TNFα treatment

LL/2, A549, MLE12, MLE15 and primary LECs were used to determine the effect of IAV and/or TNF-a treatment. The experiments were done in 96well plates. In 100 µl 10 000 cells/well were seeded out for the A549, MLE12, MLE15 and primary LECs. For the LL/2 cells 5000 cells/well were seeded out.

On the following day, the IAV was used 10:1 for A549, 1:1 for A549, LL/2, MLE12, MLE15 and 1:10 for LL/2, MLE12, MLE15 and primary LECs. All cells were infected with IAV for 24h before the lyses solution was added.

	Flu 10:1/1:1/1:10			Flu 1:1/1:10/1:20			No flu + 50µl *Medium*			No flu/No TNFα + 100 µl *Medium*		
A												
B												
C												
D												
E										Only *Medium* Background control		
F												
G										Lysis Solution Positive control		
H	No TNFα + 50µl *Medium*			No TNFα + 50µl *Medium*			No TNFα + 50µl *Medium*					

Figure 31: different setups used for analyzing the impact of IAV and TNFα on the cell death of different cell lines. Highest TNFα concentration (100ng/ml or 33ng/ml) was added in row A and was diluted 1:3 for every further row until row G.

	Flu 10:1/1:1			Flu 1:1/1:10			No flu + 50µl *Medium*			No flu/No TNFα + 100 µl *Medium*		
100ng TNFα	No TNFα + 50µl *Medium*			No TNFα + 50µl *Medium*								
+5h												
0h												
-5h												
10ng TNFα	No TNFα + 50µl *Medium*			No TNFα + 50µl *Medium*						Only *Medium* Background control		
+5h												
0h										Lysis Solution Positive control		
-5h												

Figure 30: different timings used for analyzing the impact of IAV and TNFα on the cell death of cell lines LL/2 and A549. TNFα was added in either 100ng/ml or 10ng/ml concentrations. The addition of TNFα occurred either 5 hours before the virus infection (-5h), at the same time as the virus infection (0h) or 5 hours after the virus infection (+5h).

Murine TNFα (Sigma) was added 5h after the IAV infection. It was used in different concentrations starting at 100ng/ml and going down in 1:3 steps for A549, LL/2 and

primary LECs. For MLE12 and MLE15 the used TNFα concentration started at 33ng/ml and went down in 1:3 steps (Figure 31). For LL/2 and A549 cells additional timings of TNFα were used. TNFα was added 5 hours before, at the same time and 5 hours after the IAV infection (Figure 30).

Murine TNFα (Sigma):   10ug/ml Stock

Keep at -20°C

7.6.2 Analysing the impact of zinc on the amount of cell death from IAV and/or TNFα treatment

The cell lines LL/2 and A549 were used to determine the impact of zinc on the effect of IAV and/or TNFα. Experiments were done in 96well plates. In 100μl, 10 000 cells/well were seeded out for the A549 and 5000 cells/well were seeded out for the LL/2 cell line. On the following day, the IAV was added in 10:1 (for the A549) or 1:1 (for the LL/2) concentration. The cells were incubated for 24h at 37°C before lyses solution was added.

	Flu 10:1/1:1 + 50µl *Medium*			Flu 1:1/1:10 + 0,05mM zinc			0,05mM zinc + TNFα			TNFα + 50µl *Medium*		
A												
B												
C												
D												
E												
F												
No TNFα												
H	Lysis Solution Positive control			Only *Medium* Background control						No flue/No TNFα + 100 µl *Medium*		

Figure 32: Zinc, IAV and TNFα were used in different combinations on the cell lines LL/2 and A549. Highest TNFα concentration (100ng/ml) was added in row A and was diluted 1:3 for every further row until row F.

Murine TNFα (Sigma) was added 5h after the IAV infection. It was used in different concentrations starting at 100ng/ml and going down in 1:3 steps. Zinc was added either the night before the IAV infection or at the same time as the IAV infection (Figure 32). When zinc was added the night before the IAV infection, rows which had only flu (green) and only TNFα (blue) the medium was exchanged to normal DMEM + 10% FCS before the infection with IAV.

1mM zinc (Merck):   0,7mg   zinc   sulphate heptahydrate

                             50ml DMEM + 10FCS

                             Sterile Filtered

7.6.3 Evaluating the LDH-Assay (45)

50µl of the supernatant of each well of the 96-well plate was transferred into a new 96-well plate. 50µl of the mixture of Assay Buffer and Substrate mix was added to each well and kept in the dark at RT for 30 minutes. After that 50µl of stop solution was added.

The absorbance was measured at 492nm for 0,1s/well with the Wallac Victor^2 1420 Multilabel counter (Perkin Elmer). The data was exported from Wallace workstation to be analysed in Microsoft Excel.

The average background from the medium was subtracted from all other wells. Now the following equation was used to determine the amount of cell death per well:

$$\frac{\text{Well} - \text{untreated cells}}{\text{Max lysis} - \text{untreated cells}} \times 100$$

7.7 ELISA

We used a commonly available sandwich ELISA (DuoSet, RnDSystems) to measure the supernatants of LL/2, A549 cells alone and from the combined phagocytosis assay. The absorbance was measured at 450nm for 0,1s/well with the Wallac Victor^2 1420 Multilabel counter (Perkin Elmer). The data was exported from Wallace workstation to be analysed in Microsoft Excel.

7.7.1 TNFα

The cell lines LL/2 and A549 were tested for TNFα. The supernatant was taken after 24h IAV infection with the doses of 10:1/1:1 for A549 or 1:1/1:10 for LL/2. The supernatant was then frozen at -80°C until further use.

7.7.2 IL-10

All wells of the 6-well plate from combination points 1h, 2h and 4h of the phagocytosis assay were tested for IL-10. The Supernatant was taken at the end of the combination time. It was then spun down at 14000rpm for 90 seconds to get rid of any cell debris. The supernatant was transferred into a new eppendorf tube and frozen at -80°C until further use.

7.8 Flow cytometry (FCM)

The used machine was a FACS Calibur (Becton Dickins) with 2 emission spectra of 488nm and 635nm. The fluorescent materials used were excited and detected with following channels: (62; 63)

	Exitation	Emission	Color
FACS Calibur Laser	-	488nm & 635nm	-
PI	488nm	617nm	Red (FL2/FL3)
FITC	495nm	521nm	Green (FL1)
APC	633nm	660nm	(FL4)
PE	495nm	575nm	Orange-red (FL2)
PKH26	488nm	567nm	Orange (FL2)
Cell tracker green	492nm	517nm	Green (FL1)
7aad	488nm	647nm	Red (FL3)

FL 1	530 +/- 30nm
FL 2	585 +/- 42nm
FL 3	670 Long pass
FL 4	661 +/- 16nm

The data was analysed on a Mac computer with the cell quest pro software.

FACS-Buffer: 500ml   PBS

1%   BSA

0,01% Sodium Acid

7.8.1 Measuring macrophage cell survival

Macrophages were split into 3x6 well non-tissue culture treated plates (Becton Dickins) having 3.10^5 macrophages per well. The macrophages were then infected with IAV on the same day at 17.00, on the next day at 6.00 and 11.00 with concentrations of 30:1, 10:1, 3:1, 1:1, 1:3 and uninfected.

24h after the first infection the supernatant and the cells were harvested with PBS+ 2mM EDTA. They were then spun down at 1300rpm fro 5min. After removing the supernatant the cells were resuspended in 100µl Annexin V binding Buffer (eBioscience). Then 5µl of Annexin V-FITC (eBioscience) or Annexin V-PE (eBioscience) was added and incubated for 10 minutes. An additional 200µl of Annexin V binding Buffer were added. Directly before FACS analyses 5µl of propidium Iodide were added.

7.8.2 Measuring the infection intensity with M2-AB

To prove that macrophages were infected, we took them off after the live imaging experiment using PBS+2mM EDTA. Fresh macrophages were scraped off for uninfected control. They were then spun down at 1400rpm for 5min. Supernatant was sucked off and they were washed 2 times with 1ml FACS-Buffer. The mouse monoclonal directed to Influenza A Virus M2 Protein primary AB (Abcam), was incubated for 30 minutes on ice at a dilution of 1:200. The cells were then washed 2 times with 1ml FACS-Buffer. The

APC goat anti-mouse Ig secondary AB (Becton Dickins) was incubated for 30 minutes on ice in the dark, at a dilution of 1:200. The cells were then washed one time with 1ml of FACS-Buffer. Then they were transferred to FACS-tubes in 300µl of FACS-Buffer and analyzed via FACS Calibur (Becton Dickins).

7.8.3 Phagocytic activity assay of macrophages

Macrophages were seeded out between days 10-18. Single colour controls (SCC) were seeded out for 7aad (Becton Dickins) and unstained before further staining.

For further staining with cell tracker green (Invitrogen) they were counted with Vi-Cell, Cell viability Analyzer (Beckman Coulter) to have a total of $1,1.10^7$ macrophages that were washed once in 10ml serum-free DMEM medium at 1400 rpm for 5 minutes. They were then taken up in 10ml DMEM with 0,8µl (0,8µM) cell tracker green and incubated for 30 minutes at 37°C with a rotation of 170. The cells were then centrifuged at 1400 rpm for 5 minutes and taken up in complete medium to stop the staining. They were once more centrifuged and taken up in complete medium and then incubated for 30 minutes at 37°C with a rotation of 170. Once more they were centrifuged at 1400 rpm for 5 minutes to be taken up in 1ml of complete macrophage medium. (64) They were counted 1:10 with Vi-Cell, Cell viability Analyzer (Beckman Coulter) and taken up in enough medium to have 2.10^5 cells per well of a non-tissue culture treated 6 well plate (Becton Dickins).

2ml per well were seeded out onto 3x non-tissue culture treated 6-well plates and into the 3 empty wells of the already used 6-well plate (**Figure 33**). The top rows of the plates were infected at 18^{00} with a 2:1/1:3 A/WSN/33(H1N1) strain of influenza A virus (IAV) while the lower ones stayed uninfected.

A			B		
Influenza 2:1/1:3	Influenza 2:1/1:3	Influenza 2:1/1:3	Stained influenza 2:1/1:3	Stained X	Stained SCC
X	X	X	Influenza 2:1 7aad SCC	Unstained SCC	

Figure 33: Distribution of the macrophages for the phagocytic activity assay. A: Plated out 3 times for the combination with the LL/2 cells over 3 different time periods (1h/2h/4h). B: Cell death assay and SCC stains.

The LL/2 cells were taken off by Trypsin-EDTA and counted with Vi-Cell, Cell viability Analyzer to have 5.10^5 cells per well of a 6-well multidishes (Nunc). SCCs were seeded out for 7aad and unstained. For further staining a total of 4.10^7 LL/2 cells were taken and stained with PKH26 for general cell membrane labelling (Sigma-Aldrich). The cells were once washed in 10ml serum-free DMEM medium with 1400 rpm for 5 minutes. The supernatant was carefully sucked off to leave no medium behind. 1ml Diluent C was used to resuspend the pellet thoroughly. Immediately 1ml of Diluent C with 8 µl (8µM) of PKH26 was added and left for 3

minutes while mildly inverting the tube. The reaction was stopped by adding an equal amount of FCS for 1 minute. Then an equal amount of complete medium was added and the cells were centrifuged with 1400 rpm for 10 minutes. The supernatant was sucked off and the pellet was transferred into a new tube for further washing. This was repeated 3 times. Cells were then taken up in complete medium. For the time points 4h, 2h and 1h we seeded 3.10^6 cells into 9x 35mm tissue culture treated dish (Becton Dickins) in 4ml medium (**Figure 34**). Immediately after that the dishes for influenza A virus (IAV) were infected 5:1. Etoposide treated dishes were induced with 4µl (10mM concentration) of Etoposide.

4h	2h	1h
3.10^6 cells	3.10^6 cells	3.10^6 cells

Figure 34: Setup with PKH26 labelled LL/2 cells. 3 dishes for each time point for analyses of A/WSN/33(H1N1) strain of influenza A virus (IAV) infected cells, Etoposide treated cells and untreated cells.
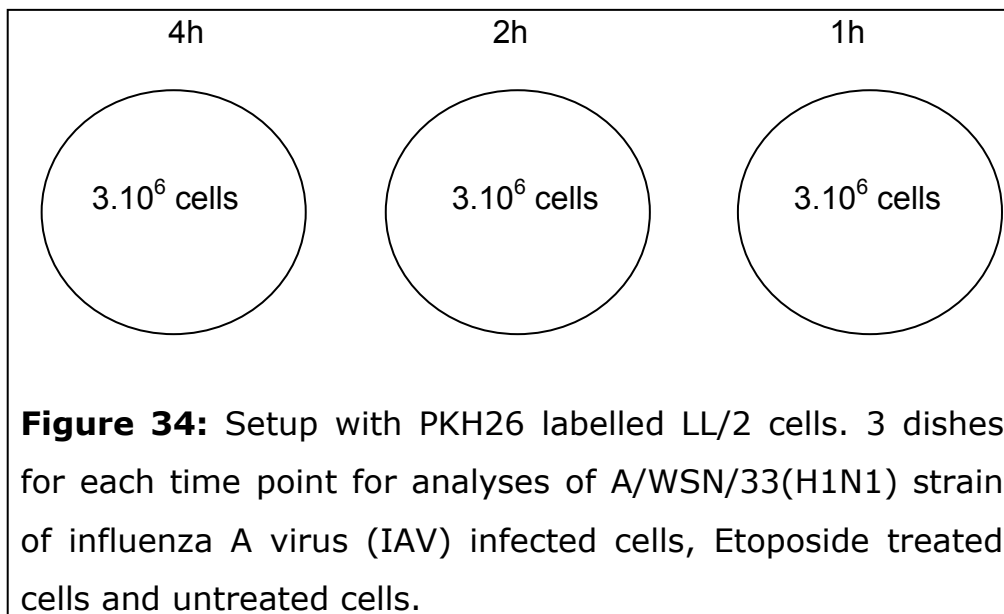
On the next day the LL/2 cells and their supernatant were collected by taking them off with PBS/EDTA. They were washed once in macrophage medium with 1400 rpm at RT for 5min and then counted with Vi-Cell in a 1:10 dilution. Approximately 1.10^6 cells were added to the macrophages.

The first 2 wells received IAV infected cells, the second 2 wells received Etoposide treated cells and the third 2 wells received the untreated samples. This procedure took place at 10^{00}(4h) and was repeated at 12^{00}(2h) and 13^{00}(1h). The LL/2 cells from the 1h time point were then also used for cell death analyses and stained SCC.

At 14^{00} the supernatant of the macrophages was sucked off and washed once with PBS. They were then taken off by incubating them with PBS/EDTA for 20min at 37°C. The cells were then spun down at 4°C with 1400rpm for 5min. They were taken up in 200µl of FACS-Buffer and transferred into a 96well V-Bottom plate. They were washed once more with FACS-Buffer and then resuspended in 100µl FACS-Buffer. 5µl 7aad was added to all wells except for non 7aad SCCs and kept at RT for 10 minutes. Cells were then transferred into small FACS-tubes with additional 200µl of FACS-Buffer and analysed via FACS Calibur (Becton Dickins).

Inverted labeling:

If PKH26 was used for macrophages, 4µl staining solution was used.

If cell tracker green was used for LL/2 cells, 1.6µl staining solution was used.

8 Figure overview

9 References

1. Fields B. Fields virology. 5. ed. Philadelphia: Wolters Kluwer Health/Lippincott Williams & Wilkins; 2007.

2. Bender BS, Small PA. Influenza: pathogenesis and host defense. Semin Respir Infect 1992 Mar;7(1):38-45.

3. Wagner R, Matrosovich M, Klenk H. Functional balance between haemagglutinin and neuraminidase in influenza virus infections. Rev. Med. Virol 2002 Jun;12(3):159-166.

4. Lakadamyali M, Rust MJ, Babcock HP, Zhuang X. Visualizing infection of individual influenza viruses. Proc Natl Acad Sci U S A 2003 Aug;100(16):9280-9285.

5. Bouvier NM, Palese P. The biology of influenza viruses. Vaccine 2008 Sep;26 Suppl 4:D49-53.

6. Cros JF, Palese P. Trafficking of viral genomic RNA into and out of the nucleus: influenza, Thogoto and Borna disease viruses. Virus Res 2003 Sep;95(1-2):3-12.

7. Kash JC, Goodman AG, Korth MJ, Katze MG. Hijacking of the host-cell response and translational control during influenza virus infection. Virus Res 2006 Jul;119(1):111-120.

8. Nayak DP, Hui EK, Barman S. Assembly and budding of influenza virus. Virus Res 2004 Dec;106(2):147-165.

9. Wang X, Shen Y, Qiu Y, Shi Z, Shao D, Chen P, Tong G, Ma Z. The non-structural (NS1) protein of influenza A virus associates with p53 and inhibits p53-mediated transcriptional activity and apoptosis. Biochem. Biophys. Res. Commun 2010 Apr;395(1):141-145.

10. Gannagé M, Dormann D, Albrecht R, Dengjel J, Torossi T, Rämer PC, Lee M, Strowig T, Arrey F, Conenello G, Pypaert M, Andersen J, García-Sastre A, Münz C. Matrix Protein 2 of Influenza A Virus Blocks Autophagosome Fusion with Lysosomes. Cell Host & Microbe 2009 Oct;6(4):367-380.

11. Rossman JS, Lamb RA. Autophagy, apoptosis, and the influenza virus

M2 protein. Cell Host Microbe 2009 Oct;6(4):299-300.

12. La Gruta NL, Kedzierska K, Stambas J, Doherty PC. A question of self-preservation: immunopathology in influenza virus infection. Immunol. Cell Biol 2007 Mar;85(2):85-92.

13. Julkunen I, Melén K, Nyqvist M, Pirhonen J, Sareneva T, Matikainen S. Inflammatory responses in influenza A virus infection. Vaccine 2000 Dec;19(Supplement 1):S32-S37.

14. Abbas A. Cellular and molecular immunology. 6. ed. Philadelphia: Saunders Elsevier; 2007.

15. Stark GR, Kerr IM, Williams BR, Silverman RH, Schreiber RD. How cells respond to interferons. Annu. Rev. Biochem 1998;67:227-264.

16. Adachi M, Matsukura S, Tokunaga H, Kokubu F. Expression of cytokines on human bronchial epithelial cells induced by influenza virus A. Int. Arch. Allergy Immunol 1997 Jul;113(1-3):307-311.

17. Chan M, Cheung C, Chui W, Tsao S, Nicholls J, Chan Y, Chan R, Long H, Poon L, Guan Y, Peiris J. Proinflammatory cytokine responses induced by influenza A (H5N1) viruses in primary human alveolar and bronchial epithelial cells. Respiratory Research 2005;6(1):135.

18. Burton DR. Antibodies in viral infection. Springer; 2001.

19. Morens DM, Taubenberger JK, Fauci AS. Predominant role of bacterial pneumonia as a cause of death in pandemic influenza: implications for pandemic influenza preparedness. J. Infect. Dis 2008 Oct;198(7):962-970.

20. Hussell T, Wissinger E, Goulding J. Bacterial complications during pandemic influenza infection. Future Microbiol 2009 Apr;4:269-272.

21. Mao H, Tu W, Liu Y, Qin G, Zheng J, Chan P, Lam K, Peiris JSM, Lau Y. Inhibition of human natural killer cell activity by influenza virions and hemagglutinin. J. Virol 2010 May;84(9):4148-4157.

22. Small C, Shaler CR, McCormick S, Jeyanathan M, Damjanovic D, Brown EG, Arck P, Jordana M, Kaushic C, Ashkar AA, Xing Z. Influenza Infection Leads to Increased Susceptibility to Subsequent Bacterial Superinfection by Impairing NK Cell Responses in the Lung. J Immunol 2010 Feb;184(4):2048-2056.

23. Hament JM, Kimpen JL, Fleer A, Wolfs TF. Respiratory viral infection

predisposing for bacterial disease: a concise review. FEMS Immunol. Med. Microbiol 1999 Dec;26(3-4):189-195.

24. Bakaletz LO. Viral potentiation of bacterial superinfection of the respiratory tract. Trends Microbiol 1995 Mar;3(3):110-114.

25. McCullers JA, Bartmess KC. Role of neuraminidase in lethal synergism between influenza virus and Streptococcus pneumoniae. J. Infect. Dis 2003 Mar;187(6):1000-1009.

26. Beadling C, Slifka MK. How do viral infections predispose patients to bacterial infections? Curr. Opin. Infect. Dis 2004 Jun;17(3):185-191.

27. McCullers JA, Rehg JE. Lethal synergism between influenza virus and Streptococcus pneumoniae: characterization of a mouse model and the role of platelet-activating factor receptor. J. Infect. Dis 2002 Aug;186(3):341-350.

28. Okamoto S, Kawabata S, Nakagawa I, Okuno Y, Goto T, Sano K, Hamada S. Influenza A virus-infected hosts boost an invasive type of Streptococcus pyogenes infection in mice. J. Virol 2003 Apr;77(7):4104-4112.

29. Slifka MK, Whitton JL. Antigen-specific regulation of T cell-mediated cytokine production. Immunity 2000 May;12(5):451-457.

30. Slifka MK, Whitton JL. Clinical implications of dysregulated cytokine production. J. Mol. Med 2000;78(2):74-80.

31. Amanda M. Jamieson, R.J.H.a.R.M. Respiratory co-infection with influenza virus and Legionella pneumophila results in rapid lethal infectious pneumonitis. 2009;

32. Vallee BL, Falchuk KH. The biochemical basis of zinc physiology. Physiol. Rev 1993 Jan;73(1):79-118.

33. Sunderman FW. The influence of zinc on apoptosis. Ann Clin Lab Sci 1995 Mar;25(2):134-142.

34. Hofmann P, Sprenger H, Kaufmann A, Bender A, Hasse C, Nain M, Gemsa D. Susceptibility of mononuclear phagocytes to influenza A virus infection and possible role in the antiviral response. J. Leukoc. Biol 1997 Apr;61(4):408-414.

35. Fink SL, Cookson BT. Apoptosis, pyroptosis, and necrosis: mechanistic description of dead and dying eukaryotic cells. Infect. Immun 2005

Apr;73(4):1907-1916.

36. Wullaert A, Heyninck K, Beyaert R. Mechanisms of crosstalk between TNF-induced NF-kappaB and JNK activation in hepatocytes. Biochem. Pharmacol 2006 Oct;72(9):1090-1101.

37. Wajant H, Pfizenmaier K, Scheurich P. Tumor necrosis factor signaling. Cell Death Differ 2003 Jan;10(1):45-65.

38. Rahman MM, McFadden G. Modulation of Tumor Necrosis Factor by Microbial Pathogens. PLoS Pathog 2006 Feb;2(2)

39. Untergasser G, Rumpold H, Plas E, Witkowski M, Pfister G, Berger P. High Levels of Zinc Ions Induce Loss of Mitochondrial Potential and Degradation of Antiapoptotic Bcl-2 Protein in in Vitro Cultivated Human Prostate Epithelial Cells. Biochemical and Biophysical Research Communications 2000 Dec;279(2):607-614.

40. Sugarman B. Zinc and infection. Rev. Infect. Dis 1983 Feb;5(1):137-147.

41. Bao S, Knoell DL. Zinc modulates airway epithelium susceptibility to death receptor-mediated apoptosis. Am. J. Physiol. Lung Cell Mol. Physiol 2006 Mar;290(3):L433-441.

42. Shankar AH, Prasad AS. Zinc and immune function: the biological basis of altered resistance to infection. Am. J. Clin. Nutr 1998 Aug;68(2 Suppl):447S-463S.

43. Truong-Tran AQ, Carter J, Ruffin RE, Zalewski PD. The role of zinc in caspase activation and apoptotic cell death. Biometals 2001 Dec;14(3-4):315-330.

44. Srivastava V, Rawall S, Vijayan VK, Khanna M. Influenza a virus induced apoptosis: inhibition of DNA laddering & caspase-3 activity by zinc supplementation in cultured HeLa cells. Indian J. Med. Res 2009 May;129(5):579-586.

45. Promega. CytoTox kit 96 Non-Radioactive Cytotoxicity Assay #TB163. [date unknown];

46. Warshamana GS, Corti M, Brody AR. TNF-alpha, PDGF, and TGF-beta(1) expression by primary mouse bronchiolar-alveolar epithelial and mesenchymal cells: tnf-alpha induces TGF-beta(1). Exp. Mol. Pathol 2001 Aug;71(1):13-33.

47. Julkunen I, Melén K, Nyqvist M, Pirhonen J, Sareneva T, Matikainen S. Inflammatory responses in influenza A virus infection. Vaccine 2000 Dec;19(Supplement 1):S32-S37.

48. Takeichi M. The cadherins: cell-cell adhesion molecules controlling animal morphogenesis. Development 1988 Apr;102(4):639-655.

49. Zitvogel L, Kepp O, Kroemer G. Decoding cell death signals in inflammation and immunity. Cell 2010 Mar;140(6):798-804.

50. Jones GE. Cellular signaling in macrophage migration and chemotaxis. J. Leukoc. Biol 2000 Nov;68(5):593-602.

51. Ehrhardt C, Ludwig S. A new player in a deadly game: influenza viruses and the PI3K/Akt signalling pathway. Cellular Microbiology 2009;11(6):863-871.

52. Zwaferink H, Stockinger S, Reipert S, Decker T. Stimulation of inducible nitric oxide synthase expression by beta interferon increases necrotic death of macrophages upon Listeria monocytogenes infection. Infect. Immun 2008 Apr;76(4):1649-1656.

53. Adler B, Adler H, Jungi TW, Peterhans E. Interferon-alpha primes macrophages for lipopolysaccharide-induced apoptosis. Biochem. Biophys. Res. Commun 1995 Oct;215(3):921-927.

54. Chen W, Calvo PA, Malide D, Gibbs J, Schubert U, Bacik I, Basta S, O'Neill R, Schickli J, Palese P, Henklein P, Bennink JR, Yewdell JW. A novel influenza A virus mitochondrial protein that induces cell death. Nat. Med 2001 Dec;7(12):1306-1312.

55. Donato NJ, Perez M. Tumor Necrosis Factor-induced Apoptosis Stimulates p53 Accumulation and p21WAF1 Proteolysis in ME-180 Cells. Journal of Biological Chemistry 1998 Feb;273(9):5067-5072.

56. Gong J, Sprenger H, Hinder F, Bender A, Schmidt A, Horch S, Nain M, Gemsa D. Influenza A virus infection of macrophages. Enhanced tumor necrosis factor-alpha (TNF-alpha) gene expression and lipopolysaccharide- triggered TNF-alpha release. J Immunol 1991 Nov;147(10):3507-3513.

57. Capsoni F, Minonzio F, Ongari A, Carbonelli V, Galli A, Zanussi C. IL-10 up-regulates human monocyte phagocytosis in the presence of IL-4 and IFN-gamma. J Leukoc Biol 1995 Sep;58(3):351-358.

58. Michlewska S, Dransfield I, Megson IL, Rossi AG. Macrophage

phagocytosis of apoptotic neutrophils is critically regulated by the opposing actions of pro-inflammatory and anti-inflammatory agents: key role for TNF-{alpha}. FASEB J. 2009 Mar;23(3):844-854.

59. Baccarini M, Bistoni F, Lohmann-Matthes ML. In vitro natural cell-mediated cytotoxicity against Candida albicans: macrophage precursors as effector cells. J. Immunol 1985 Apr;134(4):2658-2665.

60. Okuda K, Ihata A, Watabe S, Okada E, Yamakawa T, Hamajima K, Yang J, Ishii N, Nakazawa M, Okuda K, Ohnari K, Nakajima K, Xin KQ. Protective immunity against influenza A virus induced by immunization with DNA plasmid containing influenza M gene. Vaccine 2001 Jun;19(27):3681-3691.

61. Lonza. Mycoalert Mycoplasma Detection Kit. [date unknown];

62. Fluorescent Dyes for Flow Cytometric Analysis [Internet]. [date unknown];[cited 2010 Apr 16] Available from: http://www.ebioscience.com/ebioscience/appls/Dyes.htm

63. CBBC > Equipment > FACSCalibur [Internet]. [date unknown];[cited 2010 Apr 16] Available from: http://labs.pbrc.edu/cellbiology/FACSCalibur.htm

64. Krysko DV, Vanden Berghe T, Parthoens E, D'Herde K, Vandenabeele P. Methods for distinguishing apoptotic from necrotic cells and measuring their clearance. Meth. Enzymol 2008;442:307-341.

Curriculum Vitae

Personal Data

Name: Christoph Reiser

Birth date: 23.6.1984

Place of birth: Vienna, Austria

Nationality: Austria

Education

1990 – 1994   Primary school in Baden

1994 – 2002   Bundesrealgymnasium in Baden

6th of June 2002   Graduation

Jan. 02 – Sep. 2003   Military service

Since Oct. 2003   Study in Biology at University of Vienna

Since Oct. 2005   Specialization on Genetics and Microbiology

Since May 2009   Diploma Thesis at Department for Microbiology and Immunobiology at University of Vienna, under supervision of Prof. Dr. Thomas Decker, Project: The impact of Influenza A Virus on epithelial cells and macrophages

Lebenslauf

Persönliche Daten

Name:	Christoph Reiser
Birth date:	23.6.1984
Place of birth:	Wien, Österreich
Nationality:	Österreich

Ausbildung

1990 – 1994	Volksschule in Baden
1994 – 2002	Bundesrealgymnasium in Baden
6th of June 2002	Matura
Jan. 02 – Sep. 2003	Präsenzdienst
Since Oct. 2003	Studium in Biologie an der Univerität Wien
Since Oct. 2005	Spezialisierung auf Genetik und Mikrobiologie
Since May 2009	Diplomarbeit am Department für Mikrobiologie und Immunbiologie an der Universität Wien, bei Prof. Dr. Thomas Decker, Titel: The impact of Influenza A Virus on epithelial cells and macrophages